

Fig. 2. Competitive HIV-1 replication assay of HIV-1 clones in the absence of drugs. CHRA data were generated based on relative peak heights in electropherograms produced from direct DNA sequencing of HIV-1 genome at the various passages. All approximations of percentage population were made in a blinded and non-ordered manner in two or more independent assays. Representative data are shown.

predominated HIV-1_{M230I} (Fig. 2e and f), while HIV-1_{Q151L/M230I} readily predominated HIV-1_{M230I} (Fig. 2h). This was also true in contrast with the apparently comparative replicative capability of HIV-1_{Q151L/M230I} and HIV-1_{M230I} (Fig. 1c). It was also seen that HIV-1_{Q151M} outgrew HIV-1_{WT} (Fig. 2g), in agreement with our previously published data [15]. Taken together, the relative order of replication rates in the absence of drug is: HIV-1_{Q151M} > HIV-1_{WT} > HIV-1_{Q151L/M230I} > HIV-1_{M230I} >> HIV-1_{Q151L} >>> HIV-1_{Q151K}, HIV-1_{Q151F}, HIV-1_{Q151K/M230I}, HIV-1_{Q151F/M230I}.

CHRA with infectious HIV-1 clones in the presence of drugs

We also examined the replicative fitness of various molecular infectious clones in the presence of zidovudine or didanosine (Fig. 3). As expected, the drug-resistant HIV-1_{Q151M} outgrew both HIV-1_{Q151L/M230I} and HIV-1_{M230I} in the presence of zidovudine or didanosine (Fig. 3a,b,e,f). It was noted that while HIV-1_{Q151L/M230I} outgrew HIV-1_{M230I} in the presence (Fig. 3c) and absence (Fig. 2h) of 0.5 μ M zidovudine, HIV-1_{M230I} predominated over HIV-1_{Q151L/M230I} in the presence of a higher concentration of zidovudine (2 μ M) (Fig. 3d), suggesting that HIV-1_{M230I} is relatively more zidovudine-resistant than HIV-1_{Q151L/M230I}, which was not clear in the drug susceptibility assay data shown in Table 2. In the presence of didanosine (both 2 and 10 μ M), HIV-1_{Q151L/M230I} outgrew HIV-1_{M230I} (Fig. 3g), suggesting that HIV-1_{Q151L/M230I} is relatively more didanosine-resistant than HIV-1_{M230I}, in agreement with the data shown in Table 2. Thus, the comparative order

of replication rates in the presence of a lower concentration of zidovudine or didanosine is: HIV-1_{Q151M} > HIV-1_{Q151L/M230I} > HIV-1_{M230I} >>>> HIV-1_{WT}, while that in the presence of a higher concentration of zidovudine is: HIV-1_{Q151M} > HIV-1_{M230I} > HIV-1_{Q151L/M230I} >>>> HIV-1_{WT}.

Steady-state kinetic constants of various recombinant RT

Steady-state kinetic constants of RT_{WT} and mutant RT preparations were determined using p(rA) · (dT)₁₂ as a template-primer, as described previously [21]. The K_m of RT_{Q151M} was comparable to that of RT_{WT}, while those of RT_{Q151K} and RT_{Q151L} were slightly greater than that of RT_{WT} by factors of two and three, respectively (Table 3). However, the k_{cat} values of RT_{Q151K} and RT_{Q151L} were substantially less than that of RT_{WT} by factors of 0.01 and 0.08, respectively. As a result, the k_{cat}/K_m value (reflecting the catalytic efficiency) of RT_{Q151K} proved to be diminutive: only 0.6 % of that of RT_{WT} (Table 3), corroborating the detrimental replication competence of HIV-1_{Q151K}. However, the k_{cat}/K_m value of RT_{Q151L} was fivefold greater than that of RT_{Q151K}, apparently corroborating the notion that HIV-1_{Q151L} was relatively more replication-competent than HIV-1_{Q151K}. It is also noteworthy that although the K_m value of RT_{Q151L/M230I} was comparable to that of RT_{Q151L}, the k_{cat} value of the former was much greater than that of the latter, resulting in an improved k_{cat}/K_m value (0.41/sec per μ M), corroborating the observation that the acquisition of the M230I substitution improved the replication competence of HIV-1_{Q151L} (Fig. 1c).

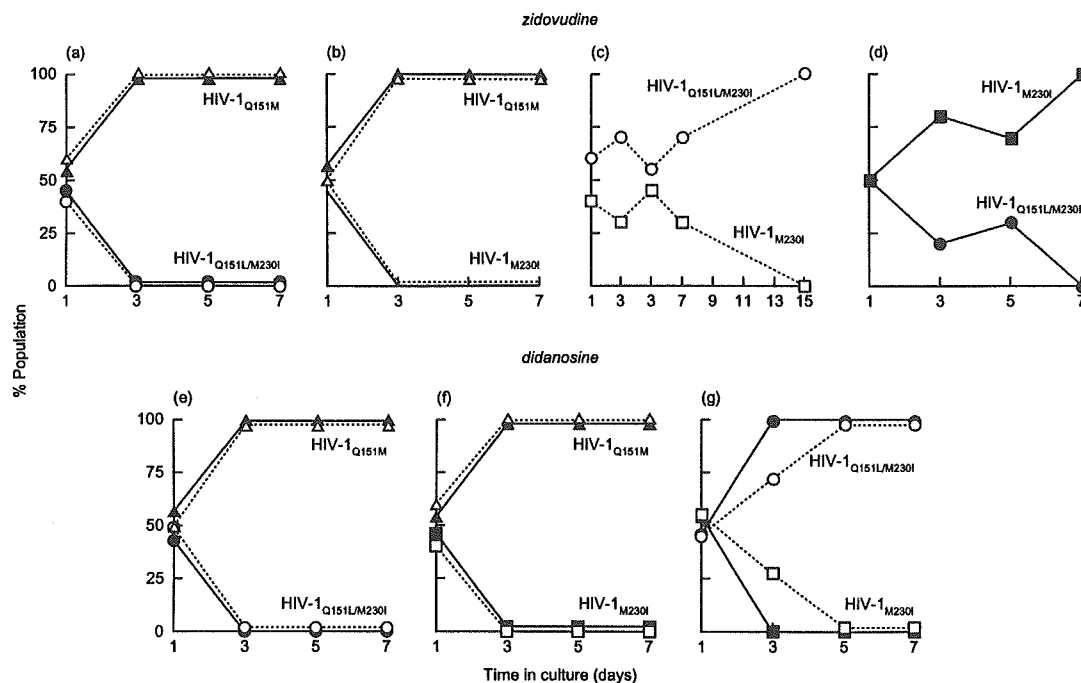


Fig. 3. Competitive HIV-1 replication assay of HIV-1 clones in the presence of drugs. CHRA data were generated as described in Fig. 2. Open symbols denote CHRA performed in the presence of low drug concentrations ($0.5 \mu\text{M}$ zidovudine and $2 \mu\text{M}$ didanosine) and filled symbols those at high drug concentrations ($2 \mu\text{M}$ zidovudine and $10 \mu\text{M}$ didanosine).

Table 3. Steady-state kinetic constants of RT_{WT} and mutant RTs. The template-primer used was p(rA) · (dT)₁₂ for determination of steady-state kinetic constants with TTP, as described in Materials and methods. Numbers in parentheses denote fold-changes compared to the values of RT_{WT}.

Enzyme	K_m (μM)	k_{cat} (/sec)	k_{cat}/K_m (/sec per μM)
RT _{WT}	0.33 ± 0.02 (1 ×)	0.65 ± 0.04 (1 ×)	2.0 (1 ×)
RT _{Q151M}	0.25 ± 0.009 (0.8 ×)	0.43 ± 0.01 (0.7 ×)	1.7 (0.8 ×)
RT _{Q151K}	0.76 ± 0.01 (2 ×)	0.009 ± 0.001 (0.01 ×)	0.012 (0.006 ×)
RT _{Q151L}	1.0 ± 0.04 (3 ×)	0.054 ± 0.006 (0.08 ×)	0.052 (0.03 ×)
RT _{Q151L/M230I}	1.1 ± 0.04 (3 ×)	0.45 ± 0.04 (0.7 ×)	0.41 (0.2 ×)
RT _{M230I}	0.75 ± 0.008 (2 ×)	0.25 ± 0.02 (0.4 ×)	0.34 (0.2 ×)

Discussion

In the present study, we attempted to elucidate the mechanism by which the HIV-1 variants resistant to multi-dideoxynucleosides emerge and the reason why their emergence is substantially delayed [6,7,10,11] compared to the appearance of HIV-1 variants resistant to other dideoxynucleosides such as zidovudine or lamivudine [23–26]. To this end, we generated a series of infectious molecular HIV-1 clones and determined their virological properties. In particular, we examined the effects of amino acid substitutions at position 151 on the replication profile of HIV-1. It is of note that the amino acid at position 151 is located in the highly conserved motif B, commonly identified in RT of various animal and human retroviruses [16] and certain mutations within this motif cause significant alterations in RT functions including the loss of enzymatic activity

[27–30]. Indeed, our previous enzymatic studies showed that the Q151M mutation induces significant alterations of RT substrate recognition [21,31]. Moreover, the recent crystallographic analyses have shown that the amino acid at position 151 is crucial for RT contact with the incoming dNTP and for the conformation of the dNTP-binding domain of RT termed the 3' pocket [14,32].

We first determined replication profiles of HIV-1_{Q151K}(AAG) and HIV-1_{Q151L}(CTG), two putative intermediates for HIV-1_{Q151M}(ATG). HIV-1_{Q151K} caused no syncytium formation or CPE and failed to propagate. In contrast, HIV-1_{Q151L} formed a low but notable level of syncytia and produced a substantial amount of p24^{agg} antigen beyond 10 days of culture (Fig. 1). In this respect, our steady-state kinetic studies revealed that the K_m values of recombinant RT_{Q151K} and RT_{Q151L}

were comparable to that of recombinant RT_{WT} (Table 3). However, the k_{cat}/K_m values of RT_{Q151K} and RT_{Q151L} were of 0.6% and 3% (for TTP) of that of RT_{WT}, respectively (Table 3). Taken together, these data suggest that HIV-1_{Q151L} replicated relatively poorly but steadily did so with its compromised but sufficiently functional RT and ultimately converted to HIV-1_{Q151M}, reverted to HIV-1_{WT}, or acquired another mutation, M230I which improved the replication capability of HIV-1_{Q151L} (Table 1). In this regard, M230I is thought to restore the compromised RT to an enzymatically more competent RT. In fact, the data have shown that the k_{cat}/K_m value of RT_{Q151L/M230I} is approximately 20% of that of RT_{WT}, presumably enabling the virus to replicate well (Table 3).

Thus, three possible pathways for HIV-1_{Q151L} to restore its replication competence were identified: (i) conversion to HIV-1_{Q151M}; (ii) reversion to HIV-1_{WT}; and (iii) the acquisition of the M230I substitution (Table 1). In terms of reversion to HIV-1_{WT}, it has also been reported that a less fit mutant virus (HIV-1_{L74V}) selected by NRTI reverts to wild type when cultured without drugs [33]. It is worth noting that M230I is located on the opposite side of Q151 in relation to the incoming dNTP, forming the 'primer grip' of RT and contacting the primer strand (Fig. 4) [14,32]. The M230I substitution has also been reported to emerge when another poorly replicative mutant clone (HIV-1_{Y115W}) was maintained in culture over an extended

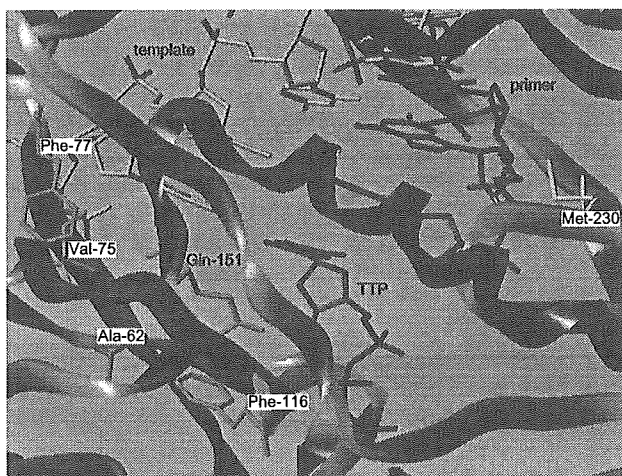


Fig. 4. The structure of the HIV-1 RT catalytic complex. A view of the RT catalytic complex with the polymerase active site, generated using SYBYL 6.7 (<http://www.tripos.com/>, Tripos Inc., St. Louis, Missouri, USA) and the coordinate set 1rtf.pdb obtained from the Protein Data Bank [14], is shown. The template, primer, and the incoming nucleotide (TTP) are depicted in cyan, purple, and orange, respectively. The five amino acids associated with the development of MDR, A62, V75, F77, F116, and Q151, are shown in green, and M230I is shown in yellow.

period of time [22]. Enzymatic studies conducted by Olivares *et al.* showed that the dNTP binding activity of the RT compromised by Y115W was compensated by the acquisition of M230I substitution and that RT_{WT} and RT_{M230I} had comparable affinity for dNTP [22], in agreement with our observation that RT_{M230I} and RT_{WT} had reasonably comparable k_{cat}/K_m values (2.0 and 0.34/sec per μM , respectively; Table 3), thereby presumably bringing about the comparable replication kinetics of HIV-1_{M230I} and HIV-1_{WT} as observed in the present study (Fig. 1c). It should be noted, however, that in CHRA assays, as expected, both HIV-1_{M230I} and HIV-1_{Q151L/M230I} were detected to be less fit than HIV-1_{WT} and HIV-1_{Q151M} in the absence of drugs and the same was true for HIV-1_{Q151M} in the presence of zidovudine or didanosine (Figs 2 and 3). Moreover, all HIV-1 clones carrying M230I were as sensitive or more sensitive to both zidovudine and didanosine than HIV-1_{WT} (Table 2). Thus, it seems unlikely that HIV-1 clones carrying M230I play a major role in the development of HIV-1_{Q151M} during antiretroviral therapy containing zidovudine and/or didanosine.

It was noted that HIV-1_{Q151L/M230I} and HIV-1_{M230I} were less sensitive to an NNRTI, nevirapine, than was HIV-1_{WT} (Table 2). In this respect, the M230L substitution has been identified commonly as the secondary mutation conferring resistance against NNRTI in a number of patients receiving them [34]. The M230I substitution has also been recently reported to Genbank (Stanford HIV RT and Protease Sequence Database, <http://hivdb.stanford.edu/>). These data endorse that the amino acid substitution at position 230 plays an important role in maintaining the enzymatic robustness in the face of multiple amino acid substitutions in the RT molecule. However, the molecular mechanism of the alterations in NNRTI sensitivity with M230I is not clear. The acquisition of M230I possibly causes conformational/functional changes to RT so that relatively compromised RT (e.g., RT_{Q151L}) might become more receptive to dideoxynucleosides but less susceptible to nevirapine. The similar phenotypic resistance reversal for NRTI has also been reported by the addition of NNRTI resistance-related mutations (L100I/K103N or L100I/Y181I) to HIV-1 carrying MDR-associated mutations, rendering the virus less resistant to dideoxynucleosides [35].

García-Lerma *et al.* recently reported that the presence of S68G, which is found in certain MDR clinical HIV-1 isolates [12,13,36], partially restored the compromised replicative competence of HIV-1_{Q151L}, suggesting that the acquisition or preexistence of S68G restores the function of RT_{Q151L} and such S68G dependence of HIV-1_{Q151L} results in the low frequency of appearance of the Q151M-mediated resistance pathway [37]. However, it is worth noting that the S68G mutation

emerged after the appearance of Q151M in all of the patients documented to date [12,13].

Our enzymatic analyses of recombinant RT_{Q151L} showed that the K_i values for RT_{Q151L} (1.8 and 4.8 μ M with zidovudine-triphosphate and ddATP, respectively) are much greater than those for RT_{WT} (0.011 and 0.23 μ M with zidovudine-triphosphate and ddATP, respectively), strongly suggesting that HIV-1_{Q151L} can propagate in the presence of zidovudine and didanosine albeit only slowly and may serve as an intermediate for HIV-1_{Q151M} (S. Harada and H. Mitsuya, unpublished data). Although the Q151L substitution has not often been identified in thus far documented clinical HIV-1 strains isolated from patients, it is likely that HIV-1_{Q151L} persists in latent reservoirs and continues to replicate slowly as seen in our experiments, constituting an undetectable HIV-1 population, and only upon Q151L conversion to Q151M, does the virus start to replicate rapidly. It should also be possible that HIV-1_{Q151M} develops through two concurrent base substitutions (CAG→ATG) at codon 151 of RT (Fig. 5). It is worth adding that HIV-1_{Q151M} is not identified in drug-naïve HIV-1-infected individuals and has occurred only in patients receiving long-term therapy with multiple NRTI such as zidovudine plus didanosine or stavudine plus didanosine, strongly suggesting that substantial as well as long-term drug selection pressure is associated with the CAG→ATG conversion.

Acknowledgments

Sponsorship: This work was supported in part by a grant from a Research for the Future Program (JSPS-RFTF 97L00705) of the Japan Society for the Promotion of Science, a Grant-in-aid for Scientific Research (Priority Areas) from the Ministry of Education, Culture, Sports, Science, and Technology of Japan (Monbu-Kagakusho), and a Grant for Promotion of AIDS Research from the

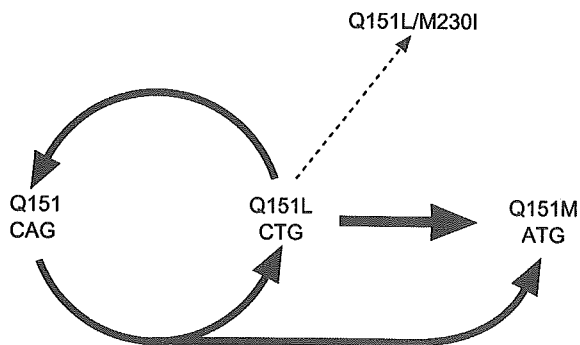


Fig. 5. Putative pathways for the emergence of HIV-1_{Q151M}. Note that the pathway shown in dots is not likely (see Discussion).

Ministry of Health, Welfare, and Labor of Japan (Kosei-Rohdoshu).

References

- Mitsuya H, Erickson J. **Discovery and development of antiretroviral therapeutics for HIV infection.** In *Textbook of AIDS Medicine, 2nd edn.* Edited by Merigan TC, Bartlet JG, Bolognesi D. Baltimore, MD: Williams & Wilkins; 1999:751–780.
- Wit FW, van Leeuwen R, Weverling GJ, Jurriaans S, Nauta K, Steingrover R, *et al.* **Outcome and predictors of failure of highly active antiretroviral therapy: one-year follow-up of a cohort of human immunodeficiency virus type 1-infected persons.** *J Infect Dis* 1999, **179**:790–798.
- Grabar S, Pradier C, Le Corfec E, Lancar R, Allavena C, Bentata M, *et al.* **Factors associated with clinical and virological failure in patients receiving a triple therapy including a protease inhibitor.** *AIDS* 2000, **14**:141–149.
- Staszewski S, Morales-Ramirez J, Tashima KT, Rachlis A, Skiest D, Stanford J, *et al.* **Efavirenz plus zidovudine and lamivudine, efavirenz plus indinavir, and indinavir plus zidovudine and lamivudine in the treatment of HIV-1 infection in adults.** *N Engl J Med* 1999, **341**:1865–1873.
- Wainberg MA, Friedland G. **Public health implications of anti-retroviral therapy and HIV drug resistance.** *JAMA* 1998, **279**:1977–1983.
- Shirasaka T, Yarchoan R, O'Brien MC, Husson RN, Anderson BD, Kojima E, *et al.* **Changes in drug sensitivity of human immunodeficiency virus type 1 during therapy with zidovudine, didoxycytidine, and didoxynosine: an in vitro comparative study.** *Proc Natl Acad Sci USA* 1993, **90**:562–566.
- Shafer RW, Kozal MJ, Winters MA, Iversen AK, Katzenstein DA, Ragni MV, *et al.* **Combination therapy with zidovudine and didanosine selects for drug-resistant human immunodeficiency virus type 1 strains with unique patterns of pol gene mutations.** *J Infect Dis* 1994, **169**:722–729.
- Winters MA, Cooley KL, Girard YA, Levee DJ, Hamdan H, Shafer RW, *et al.* **A 6-basepair insert in the reverse transcriptase gene of human immunodeficiency virus type 1 confers resistance to multiple nucleoside inhibitors.** *J Clin Invest* 1998, **102**:1769–1775.
- Brenner BG, Routy JP, Petrella M, Moisi D, Oliveira M, Detorio M, *et al.* **Persistence and fitness of multidrug-resistant human immunodeficiency virus type 1 acquired in primary infection.** *J Virol* 2002, **76**:1753–1761.
- Shirasaka T, Kavlick MF, Ueno T, Gao WY, Kojima E, Alcaide ML, *et al.* **Emergence of human immunodeficiency virus type 1 variants with resistance to multiple dideoxynucleosides in patients receiving therapy with dideoxynucleosides.** *Proc Natl Acad Sci USA* 1995, **92**:2398–2402.
- Schmit JC, Cogniaux J, Hermans P, Van Vaecq C, Sprecher S, Van Remoortel B, *et al.* **Multiple drug resistance to nucleoside analogues and nonnucleoside reverse transcriptase inhibitors in an efficiently replicating human immunodeficiency virus type 1 patient strain.** *J Infect Dis* 1996, **174**:962–968.
- Kavlick MF, Wyvill K, Yarchoan R, Mitsuya H. **Emergence of multi-dideoxynucleoside-resistant human immunodeficiency virus type 1 variants, viral sequence variation, and disease progression in patients receiving antiretroviral chemotherapy.** *J Infect Dis* 1998, **177**:1506–1513.
- Iversen AK, Shafer RW, Wehrly K, Winters MA, Mullins JJ, Chesebro B, *et al.* **Multidrug-resistant human immunodeficiency virus type 1 strains resulting from combination antiretroviral therapy.** *J Virol* 1996, **70**:1086–1090.
- Huang H, Chopra R, Verdine GL, Harrison SC. **Structure of a covalently trapped catalytic complex of HIV-1 reverse transcriptase: implications for drug resistance.** *Science* 1998, **282**:1669–1675.
- Kosalaksa P, Kavlick MF, Maroun V, Le R, Mitsuya H. **Comparative fitness of multi-dideoxynucleoside-resistant human immunodeficiency virus type 1 (HIV-1) in an in vitro competitive HIV-1 replication assay.** *J Virol* 1999, **73**:5356–5363.
- Poch O, Sauvaget I, Delarue M, Tordo N. **Identification of four conserved motifs among the RNA-dependent polymerase encoding elements.** *EMBO J* 1989, **8**:3867–3874.

17. Maeda Y, Venzon DJ, Mitsuya H. Altered drug sensitivity, fitness, and evolution of human immunodeficiency virus type 1 with pol gene mutations conferring multi-dideoxynucleoside resistance. *J Infect Dis* 1998, 177:1207–1213.
18. Reed LJ, Muench H. A simple method of estimating fifty percent endpoints. *Am J Hyg* 1938, 27:493–497.
19. Tanaka M, Srinivas RV, Ueno T, Kavlick MF, Hui FK, Fridland A, *et al.* In vitro induction of human immunodeficiency virus type 1 variants resistant to 2'-beta-Fluoro-2',3'-dideoxyadenosine. *Antimicrob Agents Chemother* 1997, 41:1313–1318.
20. Yoshimura K, Kato R, Yusa K, Kavlick MF, Maroun V, Nguyen A, *et al.* JE-2147: A dipeptide protease inhibitor (PI) that potently inhibits multi-PI-resistant HIV-1. *Proc Natl Acad Sci USA* 1999, 96:8675–8680.
21. Ueno T, Shirasaka T, Mitsuya H. Enzymatic characterization of human immunodeficiency virus type 1 reverse transcriptase resistant to multiple 2',3'-dideoxynucleoside 5'-triphosphates. *J Biol Chem* 1995, 270:23605–23611.
22. Olivares I, Sánchez-Merino V, Martínez MA, Domingo E, López-Galíndez C, Menéndez-Arias L. Second-site reversion of a human immunodeficiency virus type 1 reverse transcriptase mutant that restores enzyme function and replication capacity. *J Virol* 1999, 73:6293–6298.
23. Larder BA, Kemp SD. Multiple mutations in HIV-1 reverse transcriptase confer high-level resistance to zidovudine (AZT). *Science* 1989, 246:1155–1158.
24. Gu Z, Gao Q, Li X, Parniak MA, Wainberg MA. Novel mutation in the human immunodeficiency virus type 1 reverse transcriptase gene that encodes cross-resistance to 2',3'-dideoxyinosine and 2',3'-dideoxycytidine. *J Virol* 1992, 66:7128–7135.
25. Kellam P, Boucher CA, Larder BA. Fifth mutation in human immunodeficiency virus type 1 reverse transcriptase contributes to the development of high-level resistance to zidovudine. *Proc Natl Acad Sci USA* 1992, 89:1934–1938.
26. Schuurman R, Nijhuis M, van Leeuwen R, Schipper P, de Jong D, Collis P, *et al.* Rapid changes in human immunodeficiency virus type 1 RNA load and appearance of drug-resistant virus populations in persons treated with lamivudine (3TC). *J Infect Dis* 1995, 171:1411–1419.
27. Boyer PL, Tantillo C, Jacobo-Molina A, Nanni RG, Ding J, Arnold E, *et al.* Sensitivity of wild-type human immunodeficiency virus type 1 reverse transcriptase to dideoxynucleotides depends on template length; the sensitivity of drug-resistant mutants does not. *Proc Natl Acad Sci USA* 1994, 91:4882–4886.
28. Sarafianos SG, Pandey VN, Kaushik N, Modak MJ. Glutamine 151 participates in the substrate dNTP binding function of HIV-1 reverse transcriptase. *Biochemistry* 1995, 34:7207–7216.
29. Kaushik N, Harris D, Rege N, Modak MJ, Yadav PN, Pandey VN. Role of glutamine-151 of human immunodeficiency virus type-1 reverse transcriptase in RNA-directed DNA synthesis. *Biochemistry* 1997, 36:14430–14438.
30. Kaushik N, Talele TT, Pandey PK, Harris D, Yadav PN, Pandey VN. Role of glutamine 151 of human immunodeficiency virus type-1 reverse transcriptase in substrate selection as assessed by site-directed mutagenesis. *Biochemistry* 2000, 39:2912–2920.
31. Ueno T, Mitsuya H. Comparative enzymatic study of HIV-1 reverse transcriptase resistant to 2',3'-dideoxynucleotide analogs using the single-nucleotide incorporation assay. *Biochemistry* 1997, 36:1092–1099.
32. Sarafianos SG, Das K, Ding J, Boyer PL, Hughes SH, Arnold E. Touching the heart of HIV-1 drug resistance: the fingers close down on the dNTP at the polymerase active site. *Chem Biol* 1999, 6:R137–R146.
33. Parkina NT, Deeksb SG, Wrina MT, Yapa J, Grantc RM, Leeb KH, *et al.* Loss of antiretroviral drug susceptibility at low viral load during early virological failure in treatment-experienced patients. *AIDS* 2000, 14:2877–2887.
34. Sharma PL, Crumpacker CS. Attenuated replication of human immunodeficiency virus type 1 with a didanosine-selected reverse transcriptase mutation. *J Virol* 1997, 71:8846–8851.
35. Van Laethem K, Witvrouw M, Pannecouque C, Van Remoortel B, Schmit JC, Esnouf R, *et al.* Mutations in the non-nucleoside binding-pocket interfere with the multi-nucleoside resistance phenotype. *AIDS* 2001, 15:553–561.
36. Schmit JC, Van Laethem K, Ruiz L, Hermans P, Sprecher S, Sonnerborg A, *et al.* Multiple dideoxynucleoside analogue-resistant (MddNR) HIV-1 strains isolated from patients from different European countries. *AIDS* 1998, 12:2007–2015.
37. Garcia-Lerma JG, Gerrish PJ, Wright AC, Qari SH, Heneine W. Evidence of a role for the Q151L mutation and the viral background in development of multiple dideoxynucleoside-resistant human immunodeficiency virus type 1. *J Virol* 2000, 74:9339–9346.

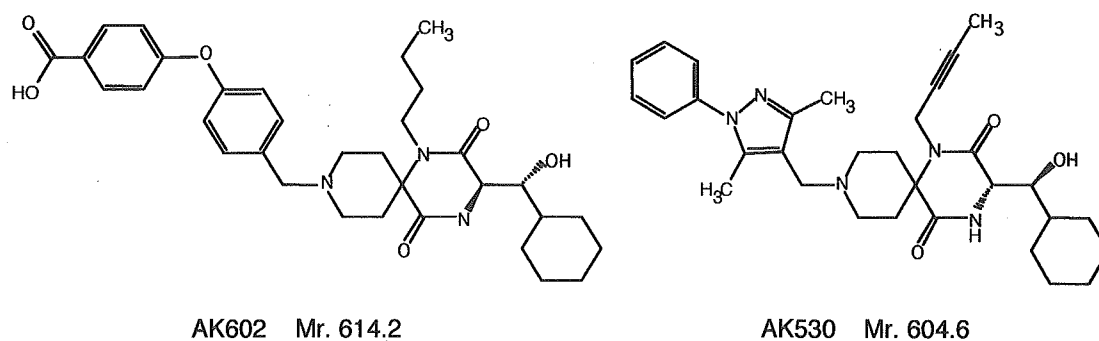


FIG. 1. Structures of AK602 and AK530.

AK671, which have the same structures as CCR5 inhibitors TAK-779 and SCH-351125 (SCH-C), respectively, were synthesized as previously described by others (1, 28).

Zidovudine was purchased from Sigma (St. Louis, Mo.). Nelfinavir and saquinavir were provided by Japan Energy (Tokyo, Japan) and Roche Products (Welwyn Garden City, United Kingdom), respectively.

¹²⁵I-labeled chemokines macrophage inflammatory protein-1 α (MIP-1 α), macrophage inflammatory protein-1 β (MIP-1 β), and RANTES were purchased from Amersham Pharmacia Biotech (Little Chalfont, United Kingdom) and PerkinElmer Life Sciences, Inc. (Boston, Mass.), and three corresponding unlabeled chemokines (MIP-1 α , MIP-1 β , and RANTES) were purchased from PepproTech Inc. (Rocky Hill, N.J.). Recombinant HIV-1_{YU2} gp120 (rgp120) and human soluble CD4 (sCD4) were purchased from Immuno Diagnostics, Inc. (Woburn, Mass.).

Cells, viruses, and anti-HIV-1 assay. Chinese hamster ovary (CHO) cells expressing CCR5 (17) were maintained in Ham's F-12 medium (Gibco-BRL, Rockville, Md.) supplemented with 10% fetal calf serum (JRH Biosciences, Lenaxa, Kans.), 50 U of penicillin per ml, and 50 μ g of streptomycin per ml in the presence of 5 μ g of blasticidin S hydrochloride per ml. Peripheral blood mononuclear cells were isolated from buffy coats of HIV-1-seronegative individuals with Ficoll-Hypaque density gradient centrifugation and cultured at a concentration of 10^6 cells/ml in RPMI 1640-based culture medium supplemented with 10% fetal calf serum and antibiotics with 10 μ g of phytohemagglutinin per ml for 3 days prior to use (phytohemagglutinin-peripheral blood mononuclear cells). Cell line CCR5⁺ MOLT4 (18) was a kind gift from Yosuke Maeda, Kumamoto University, Japan.

A panel of HIV-1 strains was employed for drug susceptibility assays: HIV 1_{Ba-L} (8), HIV-1_{JR-FL} (13) HIV-1_{NL4-3} (34), a wild-type HIV-1_{MOKW} isolated from a drug-naive AIDS patient (17), and two multidrug-resistant (HIV-1_{MDR}) primary HIV-1 strains (HIV-1_{JSL} and HIV-1_{MM}) (36). All primary HIV-1 strains were passaged once or twice in phytohemagglutinin-peripheral blood mononuclear cell cultures, and the culture supernatants were stored at -80°C until use. Antiviral assays with phytohemagglutinin-peripheral blood mononuclear cells were conducted as previously reported (12, 17, 26).

HIV-1 gp120 binding inhibition assays. CCR5⁺ CHO cells were incubated with rgp120 (5 μ g/ml) and sCD4 at 5 μ g/ml, biotinylated with EZ-link sulfo-NHS-SS-biotin (Pierce, Rockford, Ill.) in the presence of the indicated concentrations of a CCR5 inhibitor for 1 h at 37°C. Cells were washed, and the binding of the rgp120-sCD4 complex to CCR5⁺ CHO cells was determined with phycoerythrin-conjugated streptavidin (BD Pharmingen, San Diego, Calif.). Nonspecific binding was determined based on the mean fluorescence intensity of phycoerythrin-conjugated streptavidin with sCD4 but without rgp120. Drug concentrations that brought about 50% inhibition (IC₅₀) of mean fluorescence intensity were then determined.

Generation of ³H-labeled CCR5 inhibitors. Five CCR5 inhibitors, AK530, AK602, E913, E921/TAK-779, and AK671/SCH-C, were tritiated by reductive amination with sodium triacetoxyborotritide (10), methylation with [³H]methyl iodide, and heterogeneous catalytic exchange with tritium gas (4). Detailed description of the radiosynthesis of the inhibitors will be presented by J.M. elsewhere. In brief, [³H]E913, [³H]AK530, and [³H]AK602 were prepared by reductive amination of the corresponding aldehyde with piperidine-containing components of each inhibitor with an excess of sodium triacetoxyborotritide, and the tritium label was positioned selectively into the methylene group connecting the two components, generating inhibitors with specific activities of 10.2 Ci/mmol, 17.5 Ci/mmol, and 8.3 Ci/mmol, respectively. [³H]E921/TAK-779 was

prepared by methylating the *N*-methyl precursor of E921/TAK-779 with [³H]methyl iodide, generating [³H]E921/TAK-779, with a specific activity of 6.1 Ci/mmol. For the preparation of [³H]AK671/SCH-C, methyl-2,4-dimethylpyridine-3-carboxylate was tritiated by an exchange with tritium gas, catalyzed by palladium on carbon in ethanol and triethylamine. Its conversion to *N*-oxide and alkaline hydrolysis of the resulting ester provided [³H]2,4-dimethyl-pyridine-3-carboxylic acid. Its condensation with *N*-*tert*-butoxycarbonyl precursor provided [³H]AK671/SCH-C, with a specific activity of 5 Ci/mmol.

Saturation binding assay. CCR5⁺ CHO cells (1.5×10^5 cells/well) were plated onto 48-well, flat-bottomed culture plates, incubated for 24 h, rinsed with Ham's F-12 medium containing 20 mM HEPES and 0.5% bovine serum albumin (Sigma), exposed to various concentrations of each ³H-labeled CCR5 inhibitor, washed thoroughly with cold phosphate-buffered saline, and lysed with 0.5 ml of 1 N NaOH, and the radioactivity in the lysates was measured. The nonspecific binding of a radiolabeled compound was determined based on the radioactivity detected in the CCR5⁺ CHO cell-plated wells containing the same amount of the ³H-labeled CCR5 inhibitor and a 200-fold greater amount of the corresponding non radiolabeled compound. The *K_d* (dissociation) values of CCR5 inhibitors and the maximal binding values (*B_{max}* = number of CCR5/cell) were calculated based on their specific radioactivity with Graphpad Prism software (Intuitive Software for Science, San Diego, Calif.). All assays were performed in duplicate, and the values shown in this report are the arithmetic means (± 1 standard deviation) of 3 to 10 independently conducted assays.

Chemokine binding inhibition and chemotaxis inhibition assays. CCR5⁺ CHO cells (1.5×10^5) were plated onto 48-well microculture plates, incubated for 24 h, rinsed, exposed to 3 nM [¹²⁵I]MIP-1 α , [¹²⁵I]MIP-1 β , or [¹²⁵I]RANTES in the presence of various concentrations of a CCR5 inhibitor at room temperature for 1 h, thoroughly washed with phosphate-buffered saline, and lysed with 0.5 ml of 1 N NaOH, and their radioactivity was counted. The nonspecific binding of the labeled chemokine to the cells was determined based on the radioactivity detected in the wells plated with the same number of CCR5-negative CHO (CHO-K1) cells exposed to each radiolabeled chemokine (3 nM).

Chemotaxis inhibition assays were conducted with CCR5⁺ MOLT4 cells and the ChemTx System (Neuro Probe, Inc., Gaithersburg, Md.). In brief, CCR5⁺ MOLT4 cells were exposed to various concentrations of each CCR5 inhibitor for 30 min, thoroughly rinsed, plated onto the upper chamber of the ChemTx System, exposed to 0.5 nM RANTES contained in the lower chamber, and incubated for 4 h at 37°C, and the number of the cells which migrated from the upper chamber to the lower chamber was determined. Percent chemotaxis was determined with the formula $100 \times [(\text{number of CCR5 inhibitor-exposed cells which migrated to the lower chamber in the presence of RANTES}) - (\text{number of CCR5 inhibitor-unexposed cells which migrated to the lower chamber in the absence of RANTES})] / [(\text{number of CCR5 inhibitor-unexposed cells which migrated to the lower chamber in the presence of RANTES}) - (\text{number of CCR5 inhibitor-unexposed cells which migrated to the lower chamber in the absence of RANTES})]$.

FACS analysis. Fluorescence-activated cell sorting (FACS) analysis was performed as previously described (17) with minor modifications. Briefly, CCR5⁺ CHO cells (3×10^5) were stained with a phycoerythrin- or fluorescein isothiocyanate-conjugated anti-CCR5 monoclonal antibody 2D7 (BD Pharmingen, San Diego, Calif.) or 45523 or 45531 (R&D Systems, Minneapolis, Minn.), with or without a test CCR5 inhibitor, washed, and examined with an Epics XL (Beckman Coulter, Fullerton, Calif.).

RESULTS

Potent activity of AK602 against R5 wild-type and multi-drug-resistant R5 HIV-1. We have previously reported that a prototypic SDP derivative, E913, was active against R5 HIV-1 in vitro, with IC_{50} values of 30 to 60 nM as tested in target phytohemagglutinin-treated peripheral blood mononuclear cells (17). Following optimization for increased potency against R5 HIV-1 and favorable pharmacokinetic features, we identified AK602 as the most potent agent among newly designed and synthesized SDP derivatives. AK602 exerted potent activity against three wild-type R5 HIV-1 strains (HIV-1_{Ba-L}, HIV-1_{JR-FL} and HIV-1_{MOKW}) with IC_{50} values of 0.1 to 0.4 nM (Table 1). It was of note that AK602 was substantially more potent than two previously published CCR5 inhibitors, E921/TAK-779 and AK671/SCH-C (1, 28).

During the extended study of the antiviral activity of the prototypic E913, we noted that its activity against R5 HIV-1_{Ba-L} in vitro varied substantially; the range of IC_{50} values spanned from 14 to 650 nM (Fig. 2). When we tested the activity of E921/TAK-779 in phytohemagglutinin-treated peripheral blood mononuclear cells from multiple seronegative donors, its variability was also substantial: its IC_{50} values varied from 2 to 200 nM. However, when we tested AK602, the variability of AK602's anti-HIV-1 activity was limited and similar to that seen for zidovudine. The difference in the range of the CCR5 inhibitor's IC_{50} values seems to correlate with the potency of the inhibitor examined. Indeed, we have seen a greater variability in the antiviral activity of the prototypic E913 (Fig. 2). Moreover, AK602 suppressed the infectivity and replication of two HIV-1_{MDR} variants, HIV-1_{MM} and HIV-1_{JSL} (36), at extremely low concentrations (IC_{50} values of 0.4 to 0.6 nM), while these two R5 HIV-1 variants were less susceptible to zidovudine, nelfinavir, and saquinavir (IC_{50} values were greater by factors of 10 to 36, >83, and 27 to 32, respectively, compared to those against HIV-1_{Ba-L}). As expected, none of these CCR5 inhibitors suppressed the infectivity and replication of X4 HIV-1_{NL4-3} in vitro. Although certain CC-chemokines reportedly enhance the replication of X4 HIV-1 (19, 22), no such enhancement of X4 HIV-1 replication was seen with the CCR5 inhibitors examined in this study at concentrations of up to 1 μ M (data not shown).

CCR5 binding properties of SDP derivatives. We determined the CCR5 binding profiles of SDP derivatives and compared them with those of previously published CCR5 inhibitors in saturation binding assays employing ³H-labeled compounds. Figure 3A depicts the CCR5 binding profile of AK602, showing that it binds with high affinity to CCR5. The K_d values thus determined for AK602, E913, E921/TAK-779, and AK671/SCH-C were 2.9 ± 1.0 (Fig. 3A), 111.7 ± 3.5 , 32.2 ± 9.6 , and 16.0 ± 1.5 nM (data not shown), respectively.

We also asked whether the SDP derivatives blocked the binding to CCR5 of rgp120 following exposure to sCD4. As shown in Fig. 3B, AK602 potently blocked rgp120/sCD4 binding to CCR5 with an IC_{50} value of 2.7 nM, followed by E921/TAK-779 and AK-671/SCH-C, with IC_{50} values of 12.0 and 16.5 nM, respectively. When we asked whether AK602 blocked the intracellular Ca^{2+} mobilization induced by MIP-1 α , MDC, SDF-1 α , and MCP-1, whose primary receptors are CCR5, CCR4, CXCR4, and CCR2, respectively, with the method we

TABLE 1. Anti-HIV-1 activity of SDP derivatives

Compound	Mean IC_{50} (IC_{90}) \pm SD in p24 assay (nM)							CC ₅₀ ^e (μ M)
	HIV-1 _{Ba-L} (R5)	HIV-1 _{JR-FL} (R5)	HIV-1 _{MOKW} ^b (R5)	HIV-1 _{MM} ^b (R5 _{MDR})	HIV-1 _{JSL} ^b (R5 _{MDR})	HIV-1 _{NL4-3} (X4)		
AK602	0.4 \pm 0.3 (12 \pm 10)	0.1 \pm 0.1 (4 \pm 2)	0.2 \pm 0.1 (5 \pm 3)	0.6 \pm 0.2 (11 \pm 2)	0.4 \pm 0.3 (7 \pm 2)	> 1,000	50	
AK530	32 \pm 27 (324 \pm 120)	13 \pm 4 (144 \pm 60)	ND ^c	ND	ND	> 1,000	60	
E913	82 \pm 58 (709 \pm 256)	81 \pm 46 (>1,000)	51 \pm 14 (941 \pm 201)	61 \pm 28 (>1,000)	64 \pm 30 (713 \pm 405)	> 1,000	50	
E921/TAK-779	28 \pm 32 (256 \pm 169)	5 \pm 1 (237 \pm 25)	11 \pm 7 (194 \pm 168)	14 \pm 8 (352 \pm 180)	7 \pm 4 (316 \pm 151)	> 1,000	50	
AK671/SCH-C	4 \pm 2 (79 \pm 52)	2 \pm 0.5 (56 \pm 57)	2 \pm 1 (54 \pm 20)	3 \pm 0.5 (138 \pm 25)	2 \pm 0.3 (84 \pm 18)	> 1,000	> 100	
Zidovudine	7 \pm 4 (48 \pm 21)	10 \pm 9 (157 \pm 72)	6 \pm 5 (47 \pm 20)	250 \pm 98 (>1,000)	70 \pm 64 (>1,000)	11 \pm 5 (181 \pm 90)	> 100	
Nelfinavir	12 \pm 8 (105 \pm 48)	ND	14 \pm 8 (82 \pm 56)	> 1,000	> 1,000	20 \pm 7 (75 \pm 52)	ND	
Saquinavir	11 \pm 5 (60 \pm 21)	ND	5 \pm 2 (49 \pm 40)	300 \pm 65 (>1,000)	350 \pm 105 (>1,000)	10 \pm 4 (48 \pm 2)	ND	

^a Cytotoxic concentrations of a compound that reduces the number of cells by 50% (CC₅₀) were determined as previously reported (17).

^b HIV-1_{MOKW} was isolated from a drug-naïve AIDS patient (17), while HIV-1_{MM} and HIV-1_{JSL} were from patients who received antiretroviral therapy for a long period and whose virus acquired a number of mutations in the RT- and PR-encoding HIV-1 genes (36).

^c ND, not determined.

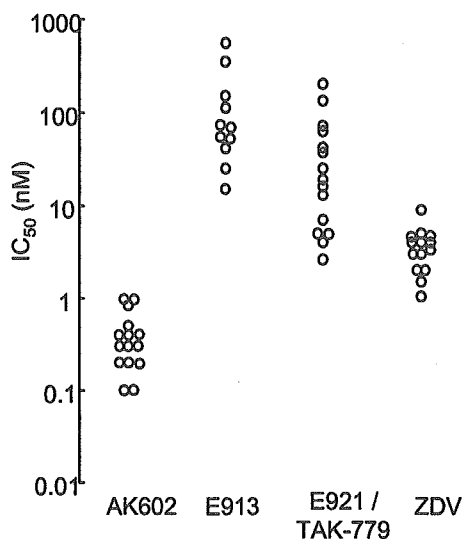


FIG. 2. Variability of anti-HIV-1 activity of AK602 in phytohemagglutinin-peripheral blood mononuclear cells. The range of IC_{50} values of E913 and E921/TAK-779 against HIV-1_{Ba-L} varied substantially when examined in multiple phytohemagglutinin-peripheral blood mononuclear cells as target cells, 14 to 650 nM ($n = 11$) and 2 to 200 nM ($n = 15$), respectively, while that of AK602 was relatively narrow, 0.1 to 1 nM ($n = 15$), similar to that of zidovudine (ZDV), 1 to 9 nM ($n = 14$).

published previously (17), AK602 completely blocked MIP-1 α -induced Ca^{2+} mobilization at 0.1 μ M and beyond; however, it failed to block Ca^{2+} mobilization induced with MDC, SDF-1 α , and MCP-1 (data not shown).

We also attempted to illustrate where AK602 binds on the

CCR5 molecule by employing several monoclonal antibodies known to bind to different domains of CCR5. FACS analyses revealed that there was no AK602 inhibition of the binding of monoclonal antibody 2D7, known to bind to the N-terminal half (or domain A) of the second extracellular loop of CCR5 (14) (Fig. 4). In contrast, AK602 competitively blocked the binding of two different monoclonal antibodies, 45523, reportedly directed against multidomain epitopes of CCR5, and 45531, which is known to be specific against the C-terminal half (or domain B) of the second extracellular loop (ECL2B) of CCR5 (14), as examined with CCR5⁺ CHO cells (Fig. 4). These data suggest that the potent activity of AK602 against R5 HIV-1 stems from its binding to ECL2B and/or its vicinity with high affinity, resulting in inhibition of gp120/CD4 binding to CCR5. It was of note, however, that another SDP derivative, AK530, whose antiviral activity was moderate (the IC_{50} value against HIV-1_{Ba-L} was 32 nM; Table 1), whose rgp120/sCD4 binding inhibition was the lowest among the inhibitors examined (IC_{50} , 280 nM; Fig. 3B), and had only a moderate effect on the binding of monoclonal antibody 45531 to CCR5⁺ cells (data not shown), had the highest binding affinity to CCR5 (K_d value, 0.4 nM; data not shown) among the SDP derivatives, suggesting that the binding pocket (or subsite) of certain SDP derivatives (such as AK530) does not quite overlap that of AK602.

SDP derivatives bind to CCR5 but permit RANTES and MIP-1 β to bind to CCR5. We asked whether SDP derivatives blocked the binding of CC-chemokines to CCR5 expressed on the surface of CHO cells with [¹²⁵I]RANTES, [¹²⁵I]MIP-1 α , and [¹²⁵I]MIP-1 β and CCR5 inhibitors AK602, AK530, E921/TAK-779, and AK671/SCH-C. As shown in Fig. 5A, the concentrations of E921/TAK-779 and AK671/SCH-C which

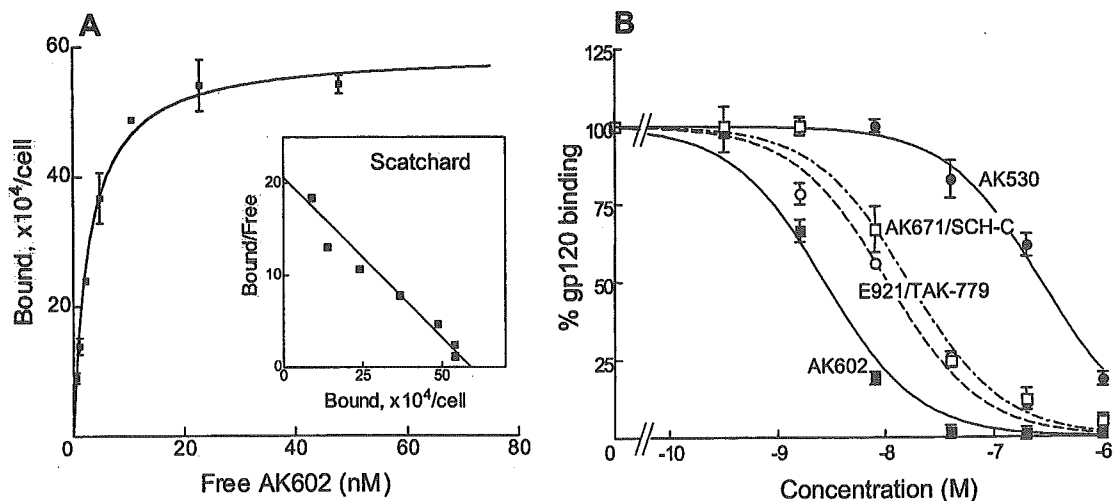


FIG. 3. CCR5 binding profiles and rgp120 binding blocking of various CCR5 inhibitors. (A) Binding affinity of AK602 to CCR5. CCR5⁺ CHO cells were incubated with the ³H-labeled CCR5 inhibitors AK530, AK602, E913, E921/TAK-779, and AK671/SCH-C for 1 h. Following thorough washing, cells were lysed, the radioactivity in the lysates was determined, and B_{max} and K_d values were calculated. The K_d values thus obtained were 0.4 ± 0.4 , 2.9 ± 1.0 , 111.7 ± 3.5 , 32.2 ± 9.6 , and 16.0 ± 1.5 nM, respectively. All assays were independently performed 3 to 10 times, and the values represent the arithmetic means \pm 1 standard deviation. (B) AK602 potently blocks the binding of rgp120/sCD4 to CCR5. CCR5⁺ CHO cells were incubated with rgp120 (5 μ g/ml) and sCD4 (5 μ g/ml) in the presence or absence of the indicated concentrations of CCR5 inhibitors, and the binding of rgp120/sCD4 complex to CCR5⁺ CHO cells was determined. The 50% binding inhibition (EC_{50}) value was determined based on the mean fluorescence intensity values obtained with or without CCR5 inhibitors. EC_{50} values for AK602, AK530, E921/TAK-779, and AK671/SCH-C were 2.7, 280, 12.0, and 16.5 nM, respectively.

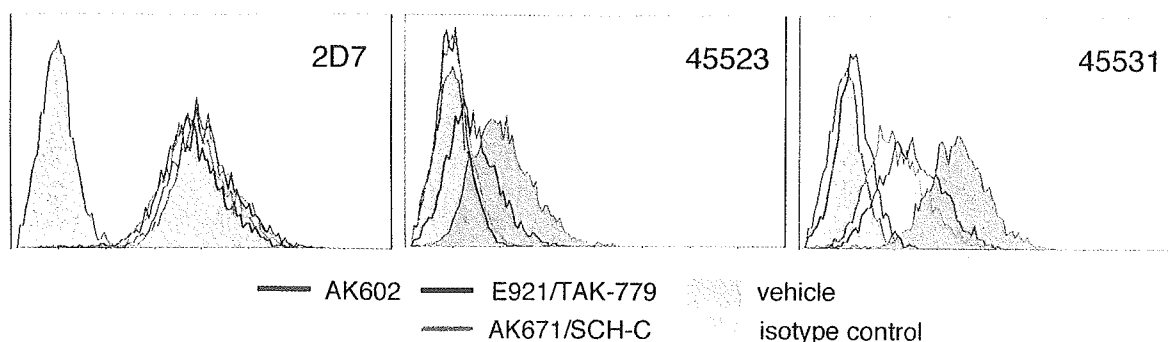


FIG. 4. AK602 binds to the second extracellular loop of CCR5. AK602 at 100 nM almost completely inhibited the binding of two monoclonal antibodies, 45523, directed against multidomain epitopes of CCR5, and 45531, recognizing ECL2B of CCR5. In contrast, E921/TAK-779 and AK671/SCH-C moderately blocked the binding of 45523 and 45531. Note that there was no AK602 inhibition of the binding of a monoclonal antibody 2D7, which is known to bind to domain A of ECL2 of CCR5.

blocked RANTES binding to CCR5 by 50% (IC_{50}) were 110 and 40 nM, respectively, and RANTES binding was completely blocked in the presence of $\geq 10 \mu\text{M}$ E921/TAK-779 or AK671/SCH-C. In contrast, AK602 only partially blocked RANTES binding to CCR5 by 40% even at $10 \mu\text{M}$ (Fig. 5A). The binding of MIP-1 β to CCR5 was also completely blocked by E921/TAK-779 and AK671/SCH-C; however, AK602 failed to completely block MIP-1 β binding (Fig. 5B). The MIP-1 β binding value in the presence of $10 \mu\text{M}$ AK602 was 10%, and no further blockade occurred at higher concentrations up to $40 \mu\text{M}$ (data not shown). AK530 also failed to completely block the binding of RANTES and MIP-1 β to CCR5.

These data suggest that the binding pockets (or subsites) of CCR5 for SDP derivatives only partially overlap the CC-chemokine binding sites of CCR5 or that the conformational changes ensuing the binding of SDP derivatives to CCR5 have only moderate effects on the binding of RANTES and MIP-1 β . In the initial search for CCR5 inhibitors, lead compounds were sought as those inhibiting MIP-1 α binding to CCR5 and MIP-1 α -driven cytosolic Ca^{2+} flux, and thus, as expected, AK602 blocked MIP-1 α binding to CCR5 although AK530 was substantially less potent in blocking MIP-1 α binding (Fig. 5C).

E921/TAK-779 and AK671/SCH-C were also found to completely block MIP-1 α binding to CCR5 (Fig. 5C).

AK602 and RANTES bind simultaneously to CCR5. As described above, AK602 and AK530 only partially inhibited RANTES binding to CCR5⁺ CHO cells; however, it was not clear whether those SDP derivatives and RANTES bound simultaneously to CCR5. Therefore, competitive binding assays employing ^3H -labeled and unlabeled AK602 and ^{125}I -labeled and unlabeled RANTES were conducted. As shown in Fig. 6A, the binding of [^3H]AK602 (10 nM) to CCR5 was only partially inhibited by ≥ 4 nM RANTES. Also, the binding of [^{125}I]RANTES at 8 nM was only inhibited by up to 20% in the presence of 10 nM AK602 (Fig. 6B).

The interpretation that AK602 and RANTES bind simultaneously to CCR5 was corroborated by another experiment in which a lower concentration of [^3H]AK602 and much higher concentrations of RANTES were used (Fig. 6A, inset). The radioactivity counted for [^3H]AK602 (5 nM) bound to CCR5⁺ CHO cells was only moderately blocked in the presence of 100 and 1,000 nM RANTES, by 32 and 46%, respectively (Fig. 6A, inset). These data suggest that the SDP derivatives, in particular AK602, and RANTES bind simultaneously to CCR5, al-

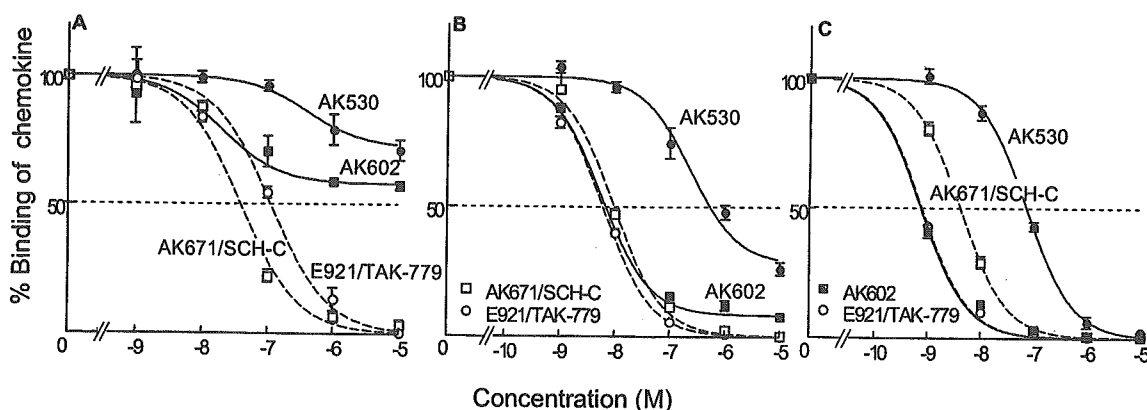


FIG. 5. Inhibition of CC-chemokine binding to CCR5 by various CCR5 inhibitors. CCR5⁺ CHO cells were incubated with 3 nM [^{125}I]RANTES (A), [^{125}I]MIP 1 β (B), or [^{125}I]MIP-1 α (Panel C) in the presence and absence of various concentrations of CCR5 inhibitors. Note that while AK671/SCH-C and E921/TAK-779 completely inhibited the binding of [^{125}I]RANTES, [^{125}I]MIP-1 α , and [^{125}I]MIP-1 β to CCR5, SDP derivatives partially blocked RANTES (A) and MIP-1 β (B) binding, although they completely blocked MIP-1 α binding (C).

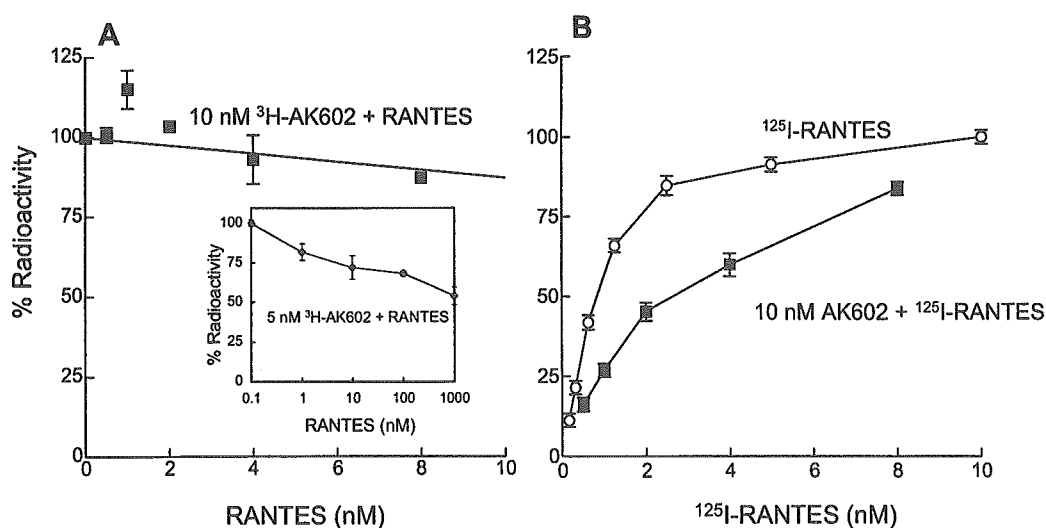


FIG. 6. AK602 and RANTES bind simultaneously to CCR5. (A) CCR5⁺ CHO cells were exposed to 10 nM [³H]AK602 and various concentrations of unlabeled RANTES. After 1 h of incubation, the cells were washed, and the [³H]AK602 bound to the cells was measured. Note that 100% radioactivity on the ordinate denotes the radioactivity of cell-bound [³H]AK602 without RANTES and that ≈90% of CCR5 molecules are bound to AK602 at 10 nM (Fig. 3A). (B) CCR5⁺ CHO cells were exposed to 10 nM unlabeled AK602 and various concentrations of [¹²⁵I]RANTES. After 1 h of incubation, the cells were washed, and the [¹²⁵I]RANTES bound to the cells was measured. The binding profile of [¹²⁵I]RANTES alone is illustrated by open circles. Note that 100% radioactivity is equated to the radioactivity of cell-bound [¹²⁵I]RANTES at 10 nM. The K_d values of RANTES in the presence and absence of 10 nM AK602 were 4.5 and 0.6 nM, respectively.

though conformational changes potentially caused by either of the two might have occurred. Indeed, 15 to 25% inhibition was seen at nearly equimolar concentrations of AK602 and RANTES, which may reflect the involvement of the conformational changes caused by either of the two agents or an overlap in their binding sites (or domains).

AK602 permits RANTES-induced chemotaxis and CCR5 internalization at anti-HIV-1 activity-exerting concentrations. We next asked whether AK602 allowed RANTES-induced chemotaxis and CCR5 internalization with CCR5⁺ MOLT4 cells and CCR5⁺ CHO cells at its anti-HIV-1 activity-exerting concentrations. As shown in Fig. 7A, AK671/SCH-C most potently blocked chemotaxis, followed by E921/TAK-779. The chemotaxis values at the IC₅₀s against R5 HIV-1_{Ba-L} of AK671/SCH-C and E921/TAK-779 (4 and 24 nM, respectively; Table 1) were low, 18 and 8%, respectively, suggesting that these two inhibitors considerably blocked chemotaxis at their anti-HIV-1 IC₅₀ concentrations as determined in peripheral blood mononuclear cells. In contrast, the chemotaxis seen at the IC₅₀ level of AK602, 0.4 nM (see Table 1), was considerable, with 70% retained (Fig. 7A), while that seen AK530 was much less (30%).

In order to corroborate the modest chemotaxis inhibition seen with AK602, the inhibition of RANTES-induced CCR5 internalization was also examined. In the absence of CCR5 inhibitors, ≈50% of CCR5 molecules were internalized from the surface of CCR5⁺ CHO cells incubated for 1 h at 37°C in the presence of 10 nM RANTES; however, AK671/SCH-C and E921/TAK-779 at 100 nM considerably blocked internalization, and only 19 and 6%, respectively, of CCR5 molecules were internalized. In the presence of higher concentrations of AK671/SCH-C and E921/TAK-779, 300 and 1,000 nM, virtually no CCR5 internalization occurred (Fig. 7B). In contrast,

AK530 and AK602 at 100 nM allowed RANTES-induced CCR5 internalization of 46 and 30%, respectively, and even at 300 and 1,000 nM, 10 to 34% CCR5 internalization occurred (Fig. 7B).

DISCUSSION

A novel SDP derivative, AK602/ONO4128/GW873140, exhibited high affinity to CCR5, blocked rgp120/sCD4 complex binding to CCR5, and exerted potent activity against a wide spectrum of laboratory and primary R5 HIV-1 isolates, including HIV-1_{MDR}. We recently examined AK602 against several non-clade B R5 HIV strains and found that in general AK602 is comparably active against such non-clade B strains (data not shown). It is of note that several small-molecule CCR5 inhibitors have been reported in the literature, including SCH-D (D. Schurmann et al., Abstr. 11th Conf. Retroviruses Opportunistic Infections, 2004, abstr. 140LB), UK427,857 (A. L. Pozniak et al. Abstr. 43rd Intersci. Conf. Antimicrob. Agents Chemother., 2003, abstr. H-443), CMPD167 (32), and TAK-220 (Y. Iizawa et al., Abstr. 10th Conf. Retroviruses Opportunistic Infections, 2003, abstr. 11).

In the present study, we also demonstrated that AK602 potently blocked rgp120/sCD4 complex binding to CCR5. With respect to gp120/CD4 binding to CCR5, Olson et al. previously reported no correlation between fusion with and entry into the target cell of HIV-1 and inhibition of rgp120/sCD4 complex binding to CCR5, based on data with various anti-CCR5 monoclonal antibodies (24). However, with all small-molecule SDP derivatives examined in the present study, inhibition of HIV-1 infectivity and replication generally correlated with inhibition of the rgp120/sCD4 complex binding to CCR5, strongly suggesting that the anti-HIV-1 activity of SDP

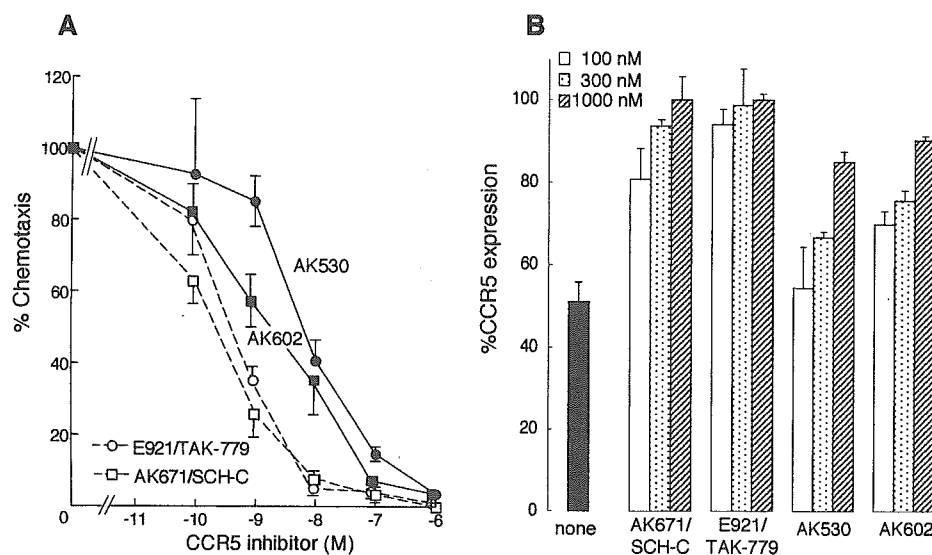


FIG. 7. AK602 allows RANTES-induced chemotaxis and CCR5 internalization. (A) CCR5⁺ MOLT4 cells were exposed to various concentrations of AK530, AK602, E921/TAK-779, or AK671/SCH-C, thoroughly washed, plated onto the upper chamber of the ChemTx System, exposed to 0.5 nM RANTES contained in the lower chamber, and incubated for 4 h; the number of the cells which migrated to the lower chamber was determined, and chemotaxis was calculated. (B) CCR5⁺ CHO cells were exposed to 10 nM RANTES in the presence or absence of various concentrations of each CCR5 inhibitor and washed with acidic solution for removal of the cell-bound RANTES (21). The amount of cell surface CCR5 was subsequently determined with monoclonal antibody 3A9 (BD PharMingen), which recognizes the N terminus of CCR5 and competes with none of the CCR5 inhibitors tested. In panel A, the level of chemotaxis suppression by TAK-779 and SCH-C was greater than that by AK530 and AK602 at four concentrations examined, although complete suppression was seen only at the highest concentration of the AK compounds, 1 μ M. However, in panel B, the level of CCR5 internalization suppression by TAK-779 and SCH-C was greater than that of the AK compounds at all three concentrations examined.

derivatives stems from their inhibition of gp120 binding to CCR5, as reported for other CCR5 inhibitors such as TAK-779 (3), although the binding pocket (or subsite) of CCR5 for certain SDP derivatives (such as AK530) apparently does not quite overlap the rgp120/sCD4 complex binding site of CCR5 (Fig. 3B). It is also possible that the conformational changes ensuing upon AK602's binding to CCR5 could differ from that ensuing upon AK530's binding to CCR5, thereby producing differences in gp120/sCD4 binding and anti-HIV activity.

It is generally noted that although the determination of any binding sites with antibodies provides "indirect" evidence, in many cases it gives good insights (14). Indeed, SCH-C has been reported to induce conformational changes in CCR5 and bind to its transmembrane (TM) domain, thereby blocking HIV-gp120 binding to CCR5. In our data, SCH-C completely blocked the binding of the "multidomain"-reactive monoclonal antibody 45523, which reportedly causes conformational changes in CCR5, while it only moderately blocked the binding of the ECL2B-specific monoclonal antibody 45531 (Fig. 4). In contrast, AK602 completely blocked the binding of both 45523 and 45531. Considering that monoclonal antibody 45531's CCR5 binding is closely linked to amino acids 184 to 189 of ECL2B, as shown by Lee and colleagues (14), it was thought that the binding site of AK602 includes ECL2B or is vicinal to it. Indeed, our recent analysis with the alanine-scanning algorithm showed that AK602 totally failed to bind to a CCR5 mutant when a K191A substitution was introduced (Maeda et al., unpublished data), corroborating and extending the idea that AK602's binding site involves the ECL2B domain.

It is noted that the IC₅₀ of AK602 against HIV-1 as deter-

mined in peripheral blood mononuclear cells (0.4, 0.1, and 0.2 nM against HIV-1_{Ba-L}, HIV-1_{JR-FL}, and HIV-1_{MOKW}, respectively; Table 1) are substantially lower than the K_d of AK602 (2.9 nM) and the IC₅₀ of AK602 for its inhibition of rgp120/sCD4 complex binding to CCR5 (2.7 nM). The anti-HIV-1 IC₅₀s of AK602 are also lower than the IC₅₀s of AK602 for its inhibition of MIP-1 α -induced Ca²⁺ influx (39.8 nM; unpublished data) and that for its inhibition of CCR5 internalization (\approx 300 nM; unpublished data).

One possible explanation for these inconsistencies is the different cell lines employed for each assay. However, it is of note that when we determined the IC₅₀ values against several R5 HIV strains and K_d values of AK602 in MAGI/CCR5 cells (18), AK602's IC₅₀s (\approx 0.2 nM) were reproducibly lower than AK602's K_d (3.8 nM) (data not shown). Thus, one can postulate that for the inhibition of HIV-1 infection by CCR5 inhibitors, not all CCR5 molecules might have to be occupied. In this regard, our studies with ³H-labeled AK602 and CD4⁺ target cells expressing CCR5, MAGI/CCR5 (18) and U373-MAGI (34), have shown that less than 30% of HIV-1 infection occurred when approximately 50% of CCR5 molecules were bound by AK602, and at its anti-HIV-1 IC₅₀ concentration, AK602 was found to bind to 5 to 20% of CCR5 molecules on the target cells (Maeda et al., unpublished data). These data suggest that when one of the multimerized CCR5 molecules is bound or occupied by AK602, inhibition of the cell is likely to be blocked, although further stoichiometric analyses need to be conducted.

It has been thought that individuals carrying a gene encoding a mutant form of CCR5 called Delta32 are resistant to HIV-1

infection and apparently do not have significant health problems (2, 15, 23, 25). One can assume that individuals with homozygous CCR5-Delta32 might inherently have certain defenses which could compensate for the deficiency of CCR5. In this regard, there has been a report that individuals carrying homozygous CCR5-Delta32 have longer survival of renal transplants than those with other genotypes, suggesting that such individuals might have compromised graft rejection immunity (7). Moreover, Woitas et al. have reported that individuals with homozygous CCR5-Delta32 have significantly higher levels of hepatitis C virus in blood than their counterparts who have wild-type CCR5, suggesting that the CCR5-Delta32 mutation may be an adverse host factor in hepatitis C virus infection (35), although others have recently argued against a role of CCR5 in susceptibility to hepatitis C virus infection or response to antiviral therapy (9). Thus, sustained, long-term suppression of the effect of CC-chemokines/CCR5 interactions, in particular in those who carry wild-type CCR5 and might not have a possible compensatory mechanism for the absence of CCR5, might produce adverse effects, and caution should be used in the development of chemokine receptor antagonists as potential therapeutics for HIV-1 infection.

In this respect, SDP derivatives such as AK602 can preserve CC-chemokine/CCR5 interactions at their anti-HIV activity-exerting concentrations; they allow RANTES and MIP-1 β binding to CCR5⁺ cells and their functions at anti-HIV-1 concentrations. In contrast, two previously published CCR5 inhibitors, TAK-779 and SCH-C, fully blocked CC-chemokine/CCR5 interactions (Fig. 5 and 7). It is of note that AK602's complete inhibition of the binding of MIP-1 α was not surprising because in the initial search of lead compounds, we sought compounds that blocked the binding of ¹²⁵I-labeled MIP-1 α to CCR5⁺ CHO cells and MIP-1 α -elicited cellular Ca²⁺ mobilization, as described previously (17).

In support of the above observation, the results of competitive binding assays with [³H]AK602 and [¹²⁵I]RANTES and their corresponding unlabeled agents clearly indicated that AK602 and RANTES bind simultaneously to CCR5 (Fig. 6). Moreover, AK602 allowed CCR5⁺ MOLT4 cells to undergo RANTES-elicited chemotaxis (Fig. 7A) and CCR5⁺ CHO cells to internalize CCR5 in response to RANTES (Fig. 7B) at concentrations much greater than AK602's anti-HIV-1 activity-exerting concentration in peripheral blood mononuclear cells. However, it is worth noting that although AK602 blocked the binding of [¹²⁵I]RANTES to CCR5⁺ CHO cells only by \approx 40% at micromolar concentrations (Fig. 5A), it virtually completely blocked the RANTES-induced chemotaxis at micromolar concentrations, as examined in CCR5⁺ MOLT4 cells (Fig. 7A). This apparent inconsistency could be explained by the different cell lines employed for each assay and the fact that the number of CCR5 molecules in CCR5⁺ CHO cells (\approx 5 \times 10⁵/cell) is substantially different from that of CCR5⁺ MOLT4 cells (\approx 1 \times 10⁵/cell), and thus, AK602 could more efficiently block the chemotaxis of MOLT4 cells. It is also possible that AK602 may more effectively block CCR5 multimerization, which is reportedly important for the functionality of the G protein-coupled receptor (29), rather than the RANTES binding block to CCR5 per se. However, it is not clear yet whether AK602's unique profile that AK602 partially allows RANTES and MIP-1 β to bind to CCR5 despite

AK602's tight binding to CCR5 brings about a clinical advantage. This can be examined only in the setting of clinical trials and careful clinical investigation in long-term treatment with such an agent.

Several HIV-1 variants which acquired resistance to CC-chemokines, including MIP-1 α and CCR5 inhibitors, have been reported. Trkola et al. described that when HIV-1 was passaged in the presence of increasing concentrations of a CCR5-specific, structurally SCH-C-related CCR5 inhibitor, AD101, an escape mutant which contained 22 amino acid substitutions in the gp120 subunits emerged as early as after 19 passages (31). This escape mutant showed a >20,000-fold resistance to AD101 and was similarly resistant to SCH-C compared with wild-type HIV-1, suggesting that HIV-1 can acquire the capability of using CCR5 bound to certain classes of CCR5 inhibitors for its entry into the target cell (31). Maeda et al. reported that HIV-1_{JR-FL}, following in vitro selection against MIP-1 α over 3 months, acquired amino acid substitutions in the V2 and V3 regions of HIV-1 gp120 and became four- to sixfold more resistant to MIP-1 α , MIP-1 β , and RANTES (18). In this regard, as of this writing, we have passaged HIV-1_{Ba-L} in CD4⁺ CCR5⁺ PM1 cells (16) in the presence of moderately increasing concentrations of AK602 in one selection experiment and aggressively increasing concentrations of AK602 in another selection experiment over 22 months (45 passages); however, the virus has acquired no detectable resistance to AK602 and no significant amino acid substitutions (Nakata et al., unpublished data).

It is worth noting that the anti-HIV-1 activity of AK602 is virtually unaffected by the presence of human serum proteins. For instance, the IC₅₀ of AK602 against HIV-1_{Ba-L} in the presence of 10% fetal calf serum in culture medium was 0.4 \pm 0.3 nM, while those of AK602 with 10 μ M α 1-acid glycoprotein and 45% human serum added to the culture medium were 0.8 \pm 0.3 and 0.7 \pm 0.7 nM, respectively. AK602 failed to induce Ca²⁺ flux, chemotaxis, or CCR5 internalization in CCR5⁺ cells (Maeda et al., unpublished data). As far as the sensitivities of our methods used in the present work, AK602 is to be categorized as a nonagonist or antagonist. The phase 1 clinical trial of AK602 in HIV-1-seronegative individuals has recently been concluded, and no significant adverse effects have been documented. Considering that AK602 potently inhibited the replication of HIV-1 in vitro and in a nonobese diabetic-SCID mouse model (Nakata et al., unpublished data) and that AK602 has a favorable oral bioavailability in rodents, averaging 20 to 30% (unpublished data), the present data strongly suggest that AK602 is a promising CCR5 inhibitor as a potential therapeutic for HIV-1 infection.

ACKNOWLEDGMENTS

We thank Steve LaFon, Larry Boone, Jim Demarest, Eddy Arnold, Shigeyoshi Harada, Kazuhisa Yoshimura, and Yosuke Maeda for helpful discussion and critical reading of the manuscript.

This work was supported in part by a grant from the Research for the Future Program (JSPS-RFTF 97L00705) of the Japan Society for the Promotion of Science, a Grant-in-Aid for Scientific Research (Priority Areas) from the Ministry of Education, Culture, Sports, Science, and Technology of Japan (Monbu-Kagakusho), and a Grant for the Promotion of AIDS Research from the Ministry of Health, Welfare, and Labor of Japan (Kosei-Rohdosh).

REFERENCES

- Baba, M., O. Nishimura, N. Kanzaki, M. Okamoto, H. Sawada, Y. Iizawa, M. Shiraiishi, Y. Aramaki, K. Okonogi, Y. Ogawa, K. Meguro, and M. Fujino. 1999. A small-molecule, nonpeptide CCR5 antagonist with highly potent and selective anti-HIV-1 activity. *Proc. Natl. Acad. Sci. USA* **96**:5698–5703.
- Dean, M., M. Carrington, C. Winkler, G. A. Huttley, M. W. Smith, R. Allikmets, J. J. Goedert, S. P. Buchbinder, E. Vittinghoff, E. Gomperts, S. Donfield, D. Vlahov, R. Kaslow, A. Saah, C. Rinaldo, R. Detels, and S. J. O'Brien. 1996. Genetic restriction of HIV-1 infection and progression to AIDS by a deletion allele of the CCR5 structural gene. Hemophilia Growth and Development Study, Multicenter AIDS Cohort Study, Multicenter Hemophilia Cohort Study, San Francisco City Cohort, ALIVE Study. *Science* **273**:1856–1862.
- Dragic, T., A. Trkola, D. A. Thompson, E. G. Cormier, F. A. Kajumo, E. Maxwell, S. W. Lin, W. Ying, S. O. Smith, T. P. Sakmar, and J. P. Moore. 2000. A binding pocket for a small molecule inhibitor of HIV-1 entry within the transmembrane helices of CCR5. *Proc. Natl. Acad. Sci. USA* **97**:5639–5644.
- Evans, E. A. 1974. Catalytic exchange in solution, p. 271–317. *In* Tritium and its compounds. Wiley and Sons, New York, N.Y.
- Fauci, A. S. 2003. HIV and AIDS: 20 years of science. *Nat. Med.* **9**:839–843.
- Finzi, D., J. Blankson, J. D. Siliciano, J. B. Margolick, K. Chadwick, T. Pierson, K. Smith, J. Lisziewicz, F. Lori, C. Flexner, T. C. Quinn, R. E. Chaisson, E. Rosenberg, B. Walker, S. Gange, J. Gallant, and R. F. Siliciano. 1999. Latent infection of CD4⁺ T cells provides a mechanism for lifelong persistence of HIV-1, even in patients on effective combination therapy. *Nat. Med.* **5**:512–517.
- Fischereder, M., B. Luckow, B. Hoehner, R. P. Wuthrich, U. Rothenpieler, H. Schneberger, U. Panzer, R. A. Stahl, I. A. Hauser, K. Budde, H. Neumayer, B. K. Kramer, W. Land, and D. Schlondorff. 2001. CC chemokine receptor 5 and renal-transplant survival. *Lancet* **357**:1758–1761.
- Gartner, S., P. Markovits, D. M. Markovitz, M. H. Kaplan, R. C. Gallo, and M. Popovic. 1986. The role of mononuclear phagocytes in HTLV-III/LAV infection. *Science* **233**:215–219.
- Glas, J., H. P. Torok, C. Simperl, A. Konig, K. Martin, F. Schmidt, M. Schaefer, U. Schiemann, and C. Folwaczny. 2003. The Delta 32 mutation of the chemokine-receptor 5 gene neither is correlated with chronic hepatitis C nor does it predict response to therapy with interferon alpha and ribavirin. *Clin. Immunol.* **108**:46–50.
- Gribble, G. W. 1975. Reactions of sodium borohydride in acidic media. Selective reduction of aldehydes with sodium triacetoborohydride. *JCS Chem. Comm.* **1975**:535–541.
- Kavlick, M. F., and H. Mitsuya. 2001. The emergence of drug-resistant human immunodeficiency virus type 1 variants and its impact on antiretroviral therapy of human immunodeficiency virus type 1 infection, p. 279–312. *In* E. de Clerq (ed.), *The art of antiretroviral therapy*. American Society for Microbiology, Washington, D.C.
- Koh, Y., H. Nakata, K. Maeda, H. Ogata, G. Bilcer, T. Devasamudram, J. F. Kincaid, P. Boross, Y. F. Wang, Y. Tie, P. Volarath, L. Gaddis, R. W. Harrison, I. T. Weber, A. K. Ghosh, and H. Mitsuya. 2003. Novel bis-tetrahydrofuranylethane-containing nonpeptidic protease inhibitor (PI) UIC-94017 (TMC114) with potent activity against multi-PI-resistant human immunodeficiency virus in vitro. *Antimicrob. Agents Chemother.* **47**:3123–3129.
- Koyanagi, Y., W. A. O'Brien, J. Q. Zhao, D. W. Golde, J. C. Gasson, and I. S. Chen. 1988. Cytokines alter production of HIV-1 from primary mononuclear phagocytes. *Science* **241**:1673–1675.
- Lee, B., M. Sharron, C. Blanpain, B. J. Doranz, J. Vakili, P. Setoh, E. Berg, G. Liu, H. R. Guy, S. R. Durell, M. Parmentier, C. N. Chang, K. Price, M. Tsang, and R. W. Doms. 1999. Epitope mapping of CCR5 reveals multiple conformational states and distinct but overlapping structures involved in chemokine and coreceptor function. *J. Biol. Chem.* **274**:9617–9626.
- Liu, R., W. A. Paxton, S. Choe, D. Ceradini, S. R. Martin, R. Horuk, M. E. MacDonald, H. Stuhlmann, R. A. Koup, and N. R. Landau. 1996. Homozygous defect in HIV-1 coreceptor accounts for resistance of some multiply-exposed individuals to HIV-1 infection. *Cell* **86**:367–377.
- Lusso, P., F. Cocchi, C. Balotta, P. D. Markham, A. Louie, P. Farci, R. Pal, R. C. Gallo, and M. S. Reitz, Jr. 1995. Growth of macrophage-tropic and primary human immunodeficiency virus type 1 (HIV-1) isolates in a unique CD4⁺ T-cell clone (PM1): failure to downregulate CD4 and to interfere with cell-line-tropic HIV-1. *J. Virol.* **69**:3712–3720.
- Maeda, K., K. Yoshimura, S. Shibayama, H. Habashita, H. Tada, K. Sagawa, T. Miyakawa, M. Aoki, D. Fukushima, and H. Mitsuya. 2001. Novel low molecular weight spirodiketopiperazine derivatives potently inhibit R5 HIV-1 infection through their antagonistic effects on CCR5. *J. Biol. Chem.* **276**:35194–35200.
- Maeda, Y., M. Foda, S. Matsushita, and S. Harada. 2000. Involvement of both the V2 and V3 regions of the CCR5-tropic human immunodeficiency virus type 1 envelope in reduced sensitivity to macrophage inflammatory protein 1alpha. *J. Virol.* **74**:1787–1793.
- Marozsan, A. J., V. S. Torre, M. Johnson, S. C. Ball, J. V. Cross, D. J. Templeton, M. E. Quinones-Mateu, R. E. Oford, and E. J. Arts. 2001. Mechanisms involved in stimulation of human immunodeficiency virus type 1 replication by aminoxy-pentane RANTES. *J. Virol.* **75**:8624–8638.
- Mitsuya, H., and J. Erickson. 1999. Discovery and development of antiretroviral therapeutics for HIV infection, p. 751–780. *In* T. C. Merigan, J. G. Bartlett, and D. Bolognesi (ed.), *Textbook of AIDS medicine*. Williams & Wilkins, Baltimore, Md.
- Miyakawa, T., K. Obaru, K. Maeda, S. Harada, and H. Mitsuya. 2002. Identification of amino acid residues critical for LD78beta, a variant of human macrophage inflammatory protein-1alpha, binding to CCR5 and inhibition of R5 human immunodeficiency virus type 1 replication. *J. Biol. Chem.* **277**:4649–4655.
- Moriuchi, H., M. Moriuchi, and A. S. Fauci. 1998. Factors secreted by human T lymphotropic virus type I (HTLV-I)-infected cells can enhance or inhibit replication of HIV-1 in HTLV-I-uninfected cells: implications for *in vivo* coinfection with HTLV-I and HIV-1. *J. Exp. Med.* **187**:1689–1697.
- O'Brien, S. J., and J. P. Moore. 2000. The effect of genetic variation in chemokines and their receptors on HIV transmission and progression to AIDS. *Immunol. Rev.* **177**:99–111.
- Olson, W. C., G. E. Rabut, K. A. Nagashima, D. N. Tran, D. J. Anselma, S. P. Monard, J. P. Segal, D. A. Thompson, F. Kajumo, Y. Guo, J. P. Moore, P. J. Maddon, and T. Dragic. 1999. Differential inhibition of human immunodeficiency virus type 1 fusion, gp120 binding, and CC-chemokine activity by monoclonal antibodies to CCR5. *J. Virol.* **73**:4145–4155.
- Samson, M., F. Libert, B. J. Doranz, J. Rucker, C. Liesnard, C. M. Farber, S. Saragosti, C. Lapoumeroulie, J. Cognaux, C. Forcellie, G. Muyldermans, C. Verhofstede, G. Burtonboy, M. Georges, T. Imai, S. Rana, Y. Yi, R. J. Smyth, R. G. Collman, R. W. Doms, G. Vassart, and M. Parmentier. 1996. Resistance to HIV-1 infection in caucasian individuals bearing mutant alleles of the CCR-5 chemokine receptor gene. *Nature* **382**:722–725.
- Shirasaka, T., M. F. Kavlick, T. Ueno, W. Y. Gao, E. Kojima, M. L. Alcaide, S. Choekijichai, B. M. Roy, E. Arnold, R. Yarchoan, and H. Mitsuya. 1995. Emergence of human immunodeficiency virus type 1 variants with resistance to multiple dideoxynucleosides in patients receiving therapy with dideoxynucleosides. *Proc. Natl. Acad. Sci. USA* **92**:2398–2402.
- Siliciano, J. D., J. Kajdas, D. Finzi, T. C. Quinn, K. Chadwick, J. B. Margolick, K. Kovacs, S. J. Gange, and R. F. Siliciano. 2003. Long term follow-up studies confirm the stability of the latent reservoir for HIV 1 in resting CD4⁺ T cells. *Nat. Med.* **9**:727–728.
- Strizki, J. M., S. Xu, N. E. Wagner, L. Wojcik, J. Liu, Y. Hou, M. Endres, A. Palani, S. Shapiro, J. W. Clader, W. J. Greenlee, J. R. Tagat, S. McCombie, K. Cox, A. B. Fawzi, C. C. Chou, C. Pugliese Sivo, L. Davies, M. E. Moreno, D. D. Ho, A. Trkola, C. A. Stoddart, J. P. Moore, G. R. Reyes, and B. M. Baroudy. 2001. SCH-C (SCH 351125), an orally bioavailable, small molecule antagonist of the chemokine receptor CCR5, is a potent inhibitor of HIV-1 infection in vitro and in vivo. *Proc. Natl. Acad. Sci. USA* **98**:12718–12723.
- Thelen, M. 2001. Dancing to the tune of chemokines. *Nat. Immunol.* **2**:129–134.
- Tsamis, F., S. Gavrilo, F. Kajumo, C. Seibert, S. Kuhmann, T. Ketas, A. Trkola, A. Palani, J. W. Clader, J. R. Tagat, S. McCombie, B. Baroudy, J. P. Moore, T. P. Sakmar, and T. Dragic. 2003. Analysis of the mechanism by which the small-molecule CCR5 antagonists SCH 351125 and SCH-350581 inhibit human immunodeficiency virus type 1 entry. *J. Virol.* **77**:5201–5208.
- Trkola, A., S. E. Kuhmann, J. M. Strizki, E. Maxwell, T. Ketas, T. Morgan, P. Pugach, S. Xu, L. Wojcik, J. Tagat, A. Palani, S. Shapiro, J. W. Clader, S. McCombie, G. R. Reyes, B. M. Baroudy, and J. P. Moore. 2002. HIV-1 escape from a small molecule, CCR5-specific entry inhibitor does not involve CXCR4 use. *Proc. Natl. Acad. Sci. USA* **99**:395–400.
- Veazey, R. S., P. J. Klasse, T. J. Ketas, J. D. Reeves, M. Piatak, Jr., K. Kunstman, S. E. Kuhmann, P. A. Marx, J. D. Lifson, J. Dufour, M. Mellford, I. Pandrea, S. M. Wolinsky, R. W. Doms, J. A. DeMartino, S. J. Siliciano, K. Lyons, M. S. Springer, and J. P. Moore. 2003. Use of a small molecule CCR5 inhibitor in macaques to treat simian immunodeficiency virus infection or prevent simian-human immunodeficiency virus infection. *J. Exp. Med.* **198**:1551–1562.
- Vodicka, M. A., W. C. Goh, L. I. Wu, M. E. Rogel, S. R. Bartz, V. L. Schweickart, C. J. Raport, and M. Emerman. 1997. Indicator cell lines for detection of primary strains of human and simian immunodeficiency viruses. *Virology* **233**:193–198.
- Westervelt, P., H. E. Gendelman, and L. Ratner. 1991. Identification of a determinant within the human immunodeficiency virus 1 surface envelope glycoprotein critical for productive infection of primary monocytes. *Proc. Natl. Acad. Sci. USA* **88**:3097–3101.
- Woitars, R. P., G. Ahlenstiel, A. Iwan, J. K. Rockstroh, H. H. Brackmann, B. Kupfer, B. Matz, R. Offergeld, T. Sauerbruch, and U. Spengler. 2002. Frequency of the HIV-protective CC chemokine receptor 5-Delta32/Delta32 genotype is increased in hepatitis C. *Gastroenterology* **122**:1721–1728.
- Yoshimura, K., R. Kato, K. Yusa, M. F. Kavlick, V. Maroun, A. Nguyen, T. Mimoto, T. Ueno, M. Shintani, J. Falloon, H. Masur, H. Hayashi, J. Erickson, and H. Mitsuya. 1999. JE-2147: a dipeptide protease inhibitor (PI) that potently inhibits multi-PI-resistant HIV-1. *Proc. Natl. Acad. Sci. USA* **96**:8675–8680.

Potent Anti-R5 Human Immunodeficiency Virus Type 1 Effects of a CCR5 Antagonist, AK602/ONO4128/GW873140, in a Novel Human Peripheral Blood Mononuclear Cell Nonobese Diabetic-SCID, Interleukin-2 Receptor γ -Chain-Knocked-Out AIDS Mouse Model

Hiroto Nakata,¹ Kenji Maeda,¹ Toshikazu Miyakawa,¹ Shiro Shibayama,²
Masayoshi Matsuo,² Yoshikazu Takaoka,² Mamoru Ito,³
Yoshio Koyanagi,^{4†} and Hiroaki Mitsuya^{1,5*}

*Department of Infectious Diseases, Kumamoto University Graduate School of Medicine, Kumamoto,¹ Ono Pharmaceutical Co. Ltd., Osaka,² Central Institute for Experimental Animals, Kawasaki,³
Department of Virology, Tohoku University Graduate School of Medicine, Sendai,⁴
Japan, and Experimental Retrovirology Section, HIV and AIDS Malignancy Branch, National Cancer Institute, Bethesda, Maryland⁵*

Received 27 May 2004/Accepted 1 October 2004

We established human peripheral blood mononuclear cell (PBMC)-transplanted R5 human immunodeficiency virus type 1 isolate JR-FL (HIV-1_{JR-FL})-infected, nonobese diabetic-SCID, interleukin 2 receptor γ -chain-knocked-out (NOG) mice, in which massive and systemic HIV-1 infection occurred. The susceptibility of the implanted PBMC to the infectivity and cytopathic effect of R5 HIV-1 appeared to stem from hyperactivation of the PBMC, which rapidly proliferated and expressed high levels of CCR5. When a novel spirodiketopiperazine-containing CCR5 inhibitor, AK602/ONO4128/GW873140 (molecular weight, 614), was administered to the NOG mice 1 day after R5 HIV-1 inoculation, the replication and cytopathic effects of R5 HIV-1 were significantly suppressed. In saline-treated mice ($n = 7$), the mean human CD4⁺/CD8⁺ cell ratio was 0.1 on day 16 after inoculation, while levels in mice ($n = 8$) administered AK602 had a mean value of 0.92, comparable to levels in uninfected mice ($n = 7$). The mean number of HIV-RNA copies in plasma in saline-treated mice were $\sim 10^6$ /ml on day 16, while levels in AK602-treated mice were 1.27×10^3 /ml ($P = 0.001$). AK602 also significantly suppressed the number of proviral DNA copies and serum p24 levels ($P = 0.001$). These data suggest that the present NOG mouse system should serve as a small-animal AIDS model and warrant that AK602 be further developed as a potential therapeutic for HIV-1 infection.

Highly active antiretroviral therapy has brought about a major impact on the AIDS epidemics in the industrially advanced nations (5, 22). However, eradication of human immunodeficiency virus type 1 (HIV-1) is thought to be currently impossible, due in part to the viral reservoirs remaining in blood and infected tissues (6). The limitation of antiviral therapy of AIDS is exacerbated by complicated regimens, the development of drug-resistant HIV-1 variants (11), and a number of inherent adverse effects (2, 31). Hence, the identification of new antiretroviral drugs that have unique mechanisms of action and produce no or minimal adverse effects remains an important therapeutic objective. In regard to development of potential anti-HIV therapies or vaccines, experimental animal models for AIDS which allow the determination of the possible efficacy of antiviral agents or vaccines have been sought since severe

combined immunodeficiency (SCID) mice engrafted with human fetal thymus, liver, or peripheral blood mononuclear cells (PBMC) were first exploited to examine antiretroviral agents (19, 25). However, a number of mouse models have suffered from false-positive and false-negative results in detecting or quantifying HIV-1 infection and replication and have required a large number of samples and mice for testing (25, 29).

In the present work, we established human PBMC-transplanted R5 HIV-1_{JR-FL}-infected, nonobese diabetic (NOD)-SCID, interleukin 2 receptor γ (IL-2R γ)-chain-knocked-out (NOG) mice, in which massive and systemic HIV-1 infection occurs, human CD4⁺/CD8⁺ cell ratios significantly decrease, and high levels of R5 HIV-1 viremia reaching as high as 10^6 copies/ml are achieved. Furthermore, we demonstrated that this unprecedented susceptibility of the implanted human PBMC to the infectivity and cytopathic effects of R5 HIV-1 infection stems from hyperactivation of the PBMC. Here, we also report a novel small nonpeptide CCR5 antagonist, AK602/ONO4128/GW873140, which exerts potent anti-HIV-1 activity in vitro against laboratory and clinical strains of HIV-1, including highly multidrug-resistant (MDR) variants.

* Corresponding author. Mailing address: Department of Infectious Diseases, Kumamoto University Graduate School of Medicine, 1-1-1 Honjo, Kumamoto 860-8556, Japan. Phone: 81-96-373-5156. Fax: 81-96-363-5265. E-mail: hmitsuya@helix.nih.gov.

† Present address: Laboratory of Viral Pathogenesis, Institute for Virus Research, Kyoto University, Kyoto 606-8507, Japan.

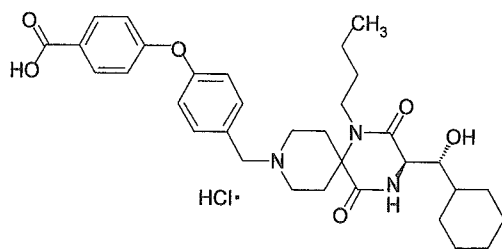


FIG. 1. Structure of AK602.

MATERIALS AND METHODS

Transplantation of human PBMC in NOG mice. NOD-SCID (NOG) mice (10, 33) were maintained in the Central Institute for Experimental Animals (Kawasaki, Japan). Mice were 4 to 6 weeks old at the time of transfer of human PBMC. The human PBMC-transplanted NOG (hu-PBMC-NOG) mice were generated by methods previously described (23, 24). Briefly, PBMC (10^7) were freshly prepared from heparinized blood of a single healthy HIV-1-seronegative donor by Ficoll-Hypaque density gradient centrifugation, resuspended in RPMI 1640-based culture medium (0.5 ml), and infused intraperitoneally to each mouse. The experimental protocol was approved by the Ethics Review Committees for Animal Experimentation of the participating institutions.

Assay for proliferation and CCR5 expression of transplanted human PBMC recovered from hu-PBMC-NOG mice. Freshly isolated human PBMC (2×10^7 cells/ml) were incubated in phosphate-buffered saline (PBS) containing $10 \mu\text{M}$ 5-carboxyfluorescein diacetate succinimidyl ester (CFSE; Molecular Probes, Eugene, Oreg.) for 15 min at 37°C for CFSE labeling as previously described by Lyons (16), washed, and resuspended in RPMI 1640. One part of the labeled PBMC preparation was intraperitoneally injected (10^7 PBMC) to each NOG mouse, and human PBMC were recovered from peritoneal lavages and spleen. The other part of the preparation was immediately stimulated with $10 \mu\text{g}$ of phytohemagglutinin (PHA)/ml, cultured, and harvested. PBMC samples thus obtained were labeled with phycoerythrin (PE)-conjugated anti-CCR5 monoclonal antibody 3A9 or peridinin chlorophyll protein-conjugated anti-HLA-DR antibody (BD Pharmingen, San Diego, Calif.) and subjected to flow cytometric analysis with a Becton Dickinson FACScan cytometer; the data were analyzed by Cell Quest software (Becton Dickinson, Franklin Lakes, N.J.). A quantitative fluorescence-activated cell sorting (FACS) assay that relies on a series of precalibrated beads that bind to a fixed number of mouse immunoglobulin G molecules (Quantum Simply Cellular Kit; Sigma, Saint Louis, Mo.) to determine the absolute number of CCR5s on the cell surface was also conducted according to the manufacturer's instructions (15).

Cells and viruses. The HeLa-CD4-LTR- β -gal indicator cell line expressing human CCR5 (CCR5⁺ MAGI) (18), a kind gift from Yosuke Maeda, was used for the present study. 293T cells (a human embryonic kidney cell line) were cultured in Dulbecco's modified Eagle medium supplemented with 10% fetal calf serum (FCS) and antibiotics and used for transfection of DNA plasmid containing the R5 HIV-1_{JR-FL} genome (13). PBMC isolated from HIV-1-seronegative individuals were cultured with 10% FCS and antibiotics with $10 \mu\text{g}$ of PHA/ml for 3 days prior to anti-HIV-1 activity assay *in vitro* (PHA-PBMC). A panel of HIV-1 strains was employed for the drug susceptibility attempt: HIV-1_{Ba-L} (7), HIV-1_{JR-FL} (13), HIV-1_{NL4.3} (32), a wild-type HIV-1_{MOKW} isolated from a drug-naïve AIDS patient (17), and MDR primary HIV-1 (HIV-1_{MDR}) strain (HIV-1_{JSL} and HIV-1_{MM}) (35). All primary HIV-1 strains were passaged once or twice in PHA-PBMC cultures and the culture supernatants were stored at -80°C until use. Antiviral assays using PHA-PBMC were conducted as previously reported (12, 17, 35).

Antiviral agents and assay for inhibition of R5 HIV-1 infectivity and replication. A series of different spirodiketopiperazine (SDP) derivatives were newly designed, synthesized, and tested for their activity against *in vitro* infectivity and replication of R5 HIV-1 as previously described (17). AK602 was chosen for this study based on its CCR5-specific, potent activity against R5 HIV-1. A method for the synthesis of AK602 will be published elsewhere. The structure of AK602 is illustrated in Fig. 1. An approved drug for therapy for HIV-1 infection, 2',3'-dideoxyinosine (ddI) (20, 21), was kindly provided by Ajinomoto Co., Inc, Tokyo, Japan. TAK779 and SCH-C were synthesized according to previously published data (1, 30). The MAGI assay using CCR5⁺ MAGI cells was conducted as previously described (17) with minor modifications. Briefly, CCR5⁺ MAGI cells were seeded in 96-well, flat-bottomed microculture plates (10^4 cells/well) for 24 h, exposed to 0.1 or $1 \mu\text{M}$ AK602 for 30 min, washed three times, exposed to

R5 HIV-1 (100 50% tissue culture infectious doses) at various time points after AK602 removal, and cultured in Dulbecco's modified Eagle medium containing 15% FCS for 48 h. Following the removal of supernatants and lysis of the cells with PBS (100 μl) containing 1% Triton X-100, a solution (100 μl) containing 10 mM chlorophenol red- β -D-galactopyranoside, 2 mM MgCl_2 , and 0.1 M KH_2PO_4 was added to each well; the mixture was incubated at room temperature in the dark for 30 min; and the optical density (wavelength, 570 nm) was measured with a microplate reader (Vmax, Molecular Devices, Sunnyvale, Calif). All assays were performed in triplicate.

Pharmacokinetic analysis of AK602 in hu-PBMC-NOG mice. Pharmacokinetic analysis of AK602 in hu-PBMC-NOG mice was performed as previously described (28). In brief, plasma samples were collected periodically over 12 h, following a single AK602 administration at a dose of 60 mg/kg of body weight dissolved in 400 μl of 4% hydroxypropyl- β cyclodextrin (HPBC). Each plasma sample (150 μl) was centrifuged at 3,000 rpm for 10 min, and the supernatant was vacuum concentrated and injected into the high-performance liquid chromatography (HPLC) system. The eluent was monitored at 255 nm of UV, and the AK602 concentration in plasma was determined.

Determination of amounts of AK602 persistently bound to CCR5 in hu-PBMC-NOG mice. Blood samples were collected from the tail vein of each hu-PBMC-NOG mouse at various time points following a single intraperitoneal administration of AK602 at a dose of 60 mg/kg. PBMC were isolated by density gradient centrifugation and stained with fluorescein isothiocyanate-conjugated monoclonal antibody 45531 (R&D Systems, Minneapolis, Minn.) specific for the C-terminal half of the second extracellular loop (ECL2B) of CCR5 (15) known to be competitively replaced by SDP derivatives (17) or with PE-conjugated monoclonal antibody 3A9, which binds to the N-terminus extracellular domain of CCR5 (17). PBMC were then subjected to FACS analysis.

Treatment of R5 HIV-1-infected hu-PBMC-NOG mice with anti-HIV-1 agents. Sixteen days after PBMC infusion, the mice were bled from the tail vein, and three-color flow cytometric analysis was performed to confirm positive engraftment of human HLA, CD4, and CD8 antigens on the cells recovered. HIV-1_{JR-FL} (2,000 50% tissue culture infectious doses) was intraperitoneally inoculated to each mouse in which PBMC engraftment was confirmed. Twenty-four hours after the R5 HIV-1 inoculation, administration of AK602 (120 mg in 4% HPBC/kg/day, twice a day), ddI (50 mg in 4% HPBC/kg/day, twice a day), or saline was implemented and continued by day 16. On days 5 and 9 after the R5 HIV-1 inoculation, blood samples were collected from mouse tail veins for immunologic and virological monitoring (see below). On day 16, blood samples were collected by cardiocentesis, and the mice were sacrificed. The experimental protocol for the treatment is illustrated in Fig. 2.

Immunologic and virological monitoring. Human PBMC recovered from mice were subjected to immunologic and virological monitoring as previously described (23, 24). The CD4⁺/CD8⁺ cell ratios were determined by FACS analysis with PE-conjugated mouse anti-CD4 and peridinin chlorophyll protein-conjugated mouse anti-CD8 (BD Pharmingen) monoclonal antibodies. Determination of HIV-1 DNA copy numbers in recovered human PBMC was performed by real-time PCR assay with Taqman Master mixture (PE Biosystems) and HIV long terminal repeat-specific primers M667 (5'-GGC TAA CTA GGG AAC CCA CTG-3') and AA55 (5'-CTG CTA GAG ATT TTC CAC ACT GAC-3'). HIV-1-specific products were quantified with the ABI 7700 detection system (Applied Biosystems, Foster City, Calif.), and cell numbers were determined with the RAG-1 gene. The numbers of CD4⁺ cells were calculated based on the percentage of CD4⁺ values obtained from the FACS analysis of each test PBMC sample, and R5 HIV-1 proviral DNA copy numbers were expressed as copy numbers per 10^5 CD4⁺ cells. In some experiments, CD4⁺ and CD4⁻ cells were separated before real-time PCR assay with the rapid immunomagnetic CD4-positive cell isolation kit (Dynabeads M-450 CD4; Dynal Biotech, Inc., Lake

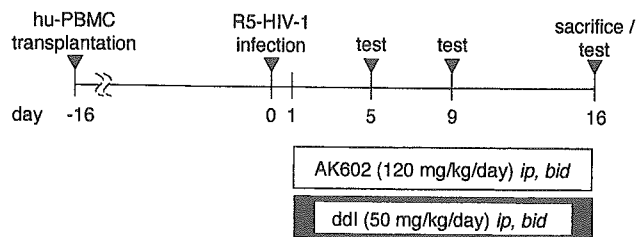


FIG. 2. Protocol for drug administration and immunological and virologic monitoring.

Success, N.Y.). The amounts of p24 antigen in murine sera were determined using a fully automated chemiluminescent enzyme immunoassay system (Lumipulse F; Fujirebio, Inc., Tokyo, Japan) as previously described (12). Plasma viral load was quantified with the AMPLICOR HIV-1 monitor test kit, version 1.5 (Roche Diagnostics, Branchburg, N.J.).

Statistical analyses. Nonparametric statistical analyses were performed by using the Mann-Whitney U test (Statview, version 5.0; Abacus Concepts, Berkeley, Calif.). The difference between viremia levels in two groups of mice was determined by the Wilcoxon rank sum test. For each mouse, the value of log₁₀ RNA copies was calculated, and the slope corresponding to the rate of increase per day was determined by simple linear regression for the days (5, 9, and 16) of blood collection. The resulting slopes for all mice in the untreated groups were compared to the slopes of mice in each of the other two groups.

RESULTS

Transplanted PBMC in hu-PBMC-NOG mice are intensely activated and express high levels of CCR5. When we examined the proliferation profile of PBMC stimulated with PHA *in vitro* by treatment with the vital dye CFSE, which allows the analysis of cell proliferation as the CFSE's fluorescence intensity is halved per each cell division, there was only a slight shift to the left in the flow cytometric profile on days 1 and 2 of culture (Fig. 3A). On day 4 of culture, a discrete shift to the left was identified, suggesting that the PHA-PBMC underwent up to four cycles of proliferation *in vitro* by day 4. In contrast, PBMC transplanted and recovered on day 2 had apparently undergone ~4 cycles of proliferation; by day 4, a majority of cells had undergone up to 10 cycles and beyond in proliferation (Fig. 3B). It was possible that the CFSE-negative and weakly CFSE-positive cells which accumulated on days 2 and 4 (Fig. 3B) were murine cells that engulfed and degraded CFSE. We therefore conducted experiments in which the cells with CFSE dilution were directly confirmed to be human CCR5-positive cells. As can be seen in Fig. 3C, when cells were recovered from the spleen of an NOG mouse into which CFSE-labeled PBMC had been transplanted and stained with monoclonal antibody 45531, which is specific for the C-terminal half of the second extracellular loop (ECL2B) of CCR5 (15), the majority of such human CCR5⁺ cells proved to be CFSE negative. We also examined the levels of cellular activation by the expression of HLA-DR on cell surface. The levels of HLA-DR expression in PBMC recovered from uninfected NOG mice 3 days after transplantation were much greater than those in 3-day-cultured PBMC following PHA stimulation (Fig. 3D). The fluorescence intensity in the same donor's PHA-PBMC examined on three different occasions was 21 ± 4 , while that of the PBMC recovered from mice was 91 ± 25 (Fig. 3D). When we further assessed the levels of CCR5 expression, the PBMC recovered from the mice on day 3 proved to be strongly positive for CCR5 (Fig. 3E). The CCR5-positive fraction in the PBMC recovered was 49.7%, while that in PHA-PBMC was 27.3%. The mean fluorescence intensity of the CCR5⁺ cell population was 141, compared to the CCR5⁺ cell population in PHA-PBMC with a mean fluorescence intensity of 51. The estimated number of CCR5 expressed on the PBMC recovered on day 3 was 25,348 (as antibody binding sites per cell) while that on PHA-PBMC on day 3 in culture was 8,981 antibody binding sites as examined by quantitative FACS assay. These data indicate that the transplanted human PBMC were intensely activated and rapidly proliferating and expressed high levels of CCR5 on their cell surfaces.

Potent activity of AK602 against R5 HIV-1 *in vitro*. Among SDP derivatives we designed and synthesized, AK602 was identified to be highly potent against a broad spectrum of R5 HIV-1 strains, including MDR clinical R5 HIV-1 isolates *in vitro* with 50% inhibitory concentration (IC₅₀) values of 0.3 to 0.6 nM, although two previously published CCR5 antagonists (TAK779 and SCH-C) were substantially less potent than AK602 (Table 1). AK602 and other CCR5 antagonists failed to inhibit the replication of an X4 HIV-1 strain, HIV-1_{NL4-3}.

Pharmacokinetics of AK602 in hu-PBMC-NOG mice. We examined the pharmacokinetics of AK602 in hu-PBMC-NOG mice by intraperitoneally administering the compound at a dose of 60 mg/kg. Plasma samples were collected periodically up to 12 h and subjected to HPLC analysis. As shown in Fig. 4A, the concentration of AK602 reached the maximal concentration immediately after intraperitoneal administration and decreased rapidly. The calculated plasma half-life in the α -phase of the concentration curve was as short as 29 min.

AK602 persists on cell surface CCR5. As shown above, the plasma half-life of AK602 turned out to be short; however, considering that AK602 possesses such a high affinity to CCR5 and potent activity against R5 HIV-1 *in vitro*, it was thought possible that AK602 would remain attached on cellular CCR5 for an extensive period of time and exert anti-R5 HIV-1 activity even when the compound was depleted from circulation. To examine this possibility, we used two monoclonal antibodies, 45531 and 3A9. When human PBMC were recovered from a hu-PBMC-NOG mouse 2 and 6 h after AK602 administration (60 mg/kg) and stained with 45531, AK602 proved to block the binding of 45531 to CCR5 (Fig. 4B), while AK602 failed to block 3A9 binding to CCR5 (Fig. 4C), suggesting that AK602 did not elicit CCR5 internalization or shedding at all at least for 6 h. We subsequently examined whether AK602 remained on cellular CCR5 with the 45531 monoclonal antibody. When the cells were recovered from mice 2, 6, and 14 h after the AK602 administration, the mean values of the percentage of AK602 occupancy were 85 (four mice), 54 (three mice), and 16 (three mice), respectively. It was calculated that it took about 9 h for AK602 occupancy to be reduced by 50% (Fig. 4D).

Anti-R5 HIV-1 activity of AK602 persistently seen after its removal from culture medium. In another depletion experiment, we exposed CCR5⁺ MAGI cells to AK602 for 30 min, depleted the compound from the culture by thorough washing, incubated the cells for various lengths of time, exposed the cells to HIV-1_{Ba-L}, further cultured the cells for 48 h, and determined whether HIV-1_{Ba-L} infection was blocked by AK602 exposure (Fig. 4E). When the CCR5⁺ MAGI cells were exposed to 0.1 and 1 μ M AK602 and exposed to HIV-1_{Ba-L} immediately afterward, the values for protection were 68 and 85%, respectively. When the cells were exposed to HIV-1_{Ba-L} 4 h after depletion, 49 and 72% of the cells were protected by 0.1 and 1 μ M AK602. When the cells were exposed to HIV-1_{Ba-L} 12 and 24 h after depletion, 57 and 45% of the cells were seen protected by 1 μ M, respectively (Fig. 4E).

Effects of AK602 on CD4⁺ and CD8⁺ cell counts in R5 HIV-1-infected hu-PBMC-NOG mice. PBMC were recovered from murine blood samples collected on days 5, 9, and 16 after R5 HIV-1 inoculation and subjected to flow cytometric analysis for determination of CD4⁺/CD8⁺ cell ratios. As shown in Fig. 5A, in PBMC recovered on day 16 from a representative

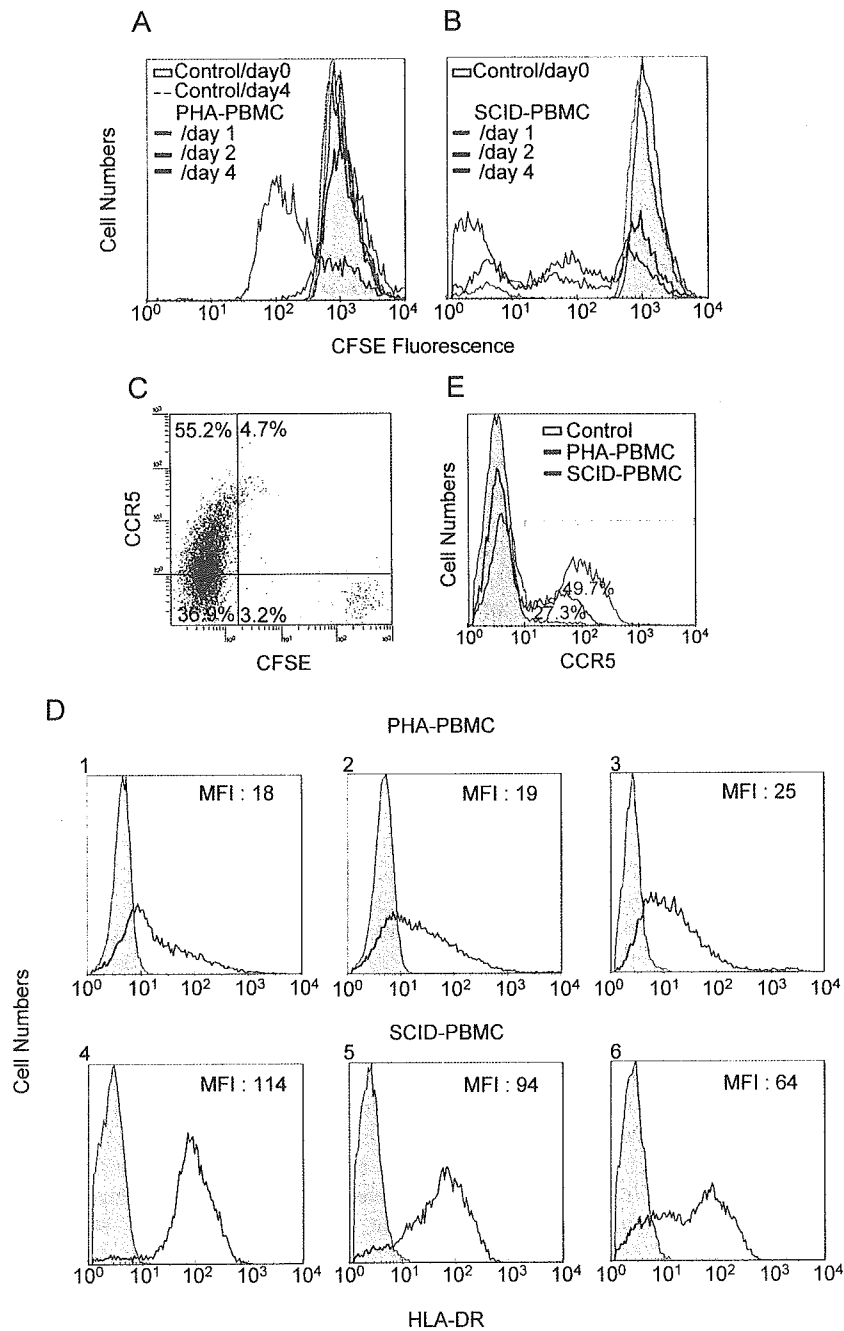


FIG. 3. Transplanted PBMC are intensely activated and express high levels of CCR5. (A and B) Proliferation profiles of PHA-PBMC and transplanted and recovered PBMC. Freshly prepared PBMC were incubated with the vital dye CFSE, and one part of such PBMC preparation was stimulated with PHA, while the other part was intraperitoneally transplanted to mice. On days 1, 2, and 4, the cells were harvested and the fluorescence intensity of CFSE was determined. Note that transplanted PBMC recovered on day 2 had undergone ~4 cycles of proliferation; by day 4, a majority of cells had undergone ~10 cycles and more of proliferation. (C) CCR5 expression level and CFSE intensity in human PBMC harvested from a spleen of hu-PBMC-NOG mouse on day 4. (D) Intense activation of PBMC after transplantation. PBMC stimulated with PHA and cultured for 4 days (panels 1 to 3) and transplanted PBMC recovered from the uninfected mice on day 4 (panels 4 to 6) were stained with an anti-HLA-DR monoclonal antibody. Note that HLA-DR expression levels in transplanted PBMC were much higher than those in PHA-PBMC. (E) CCR5 expression profiles of PHA-PBMC and transplanted PBMC. PBMC stimulated with PHA and cultured for 3 days and transplanted PBMC recovered from the uninfected mice on day 3 were stained with PE-conjugated anti-CCR5 monoclonal antibody 3A9 and subjected to flow cytometric analysis. SCID-PBMC, PBMC transplanted and recovered.

R5 HIV-1-infected, saline-treated mouse, there were only few CD4⁺ cells (3.9% [1.4% + 2.5%]) resulting in a CD4⁺/CD8⁺ cell ratio of 0.05. However, a distinct CD4⁺ cell population (55.1% [4.4% + 50.7%]) resulting in a CD4⁺/CD8⁺ ratio of

1.84 (Fig. 5B) was seen in PBMC recovered from an AK602-treated mouse, and the size of this CD4⁺ cell population was comparable to that seen in a ddI-treated mouse (53.2% [3.8% + 49.4%]) and that in an uninfected mouse (48.9% [3.8% +

TABLE 1. Anti HIV-1 activity of novel SDP derivatives in PBMC^a

Compound	IC ₅₀ value in p24 assay (nM)					
	HIV-1 _{Ba-L} (R5)	HIV-1 _{JRFL} (R5)	HIV-1 _{MOKW} (R5)	HIV-1 _{MM} (R5 _{MDR})	HIV-1 _{JSL} (R5 _{MDR})	HIV-1 _{NL4-3} (X4)
AK602	0.5 ± 0.3	0.2 ± 0.1	0.3 ± 0.2	0.7 ± 0.3	0.4 ± 0.2	>1,000
TAK779	14 ± 5	6 ± 2	9 ± 3	12 ± 4	10 ± 3	>1,000
SCH-C	3 ± 2	2 ± 1	2 ± 1.5	2.5 ± 1	2 ± 1	>1,000
ZDV	13 ± 5	7 ± 3	10 ± 6	520 ± 75	64 ± 13	9 ± 5
SQV	8 ± 3	6 ± 2	6 ± 3	212 ± 56	276 ± 44	10 ± 4

^a IC₅₀s were determined by using PHA-PBMC isolated from three different donors, and the inhibition of p24 Gag protein production was used as an endpoint. All assays were conducted in triplicate. The results shown represent arithmetic means (± standard deviation) of three independently conducted assays. HIV-1_{MOKW} was isolated from a drug-naive AIDS patient, and HIV-1_{JSL} and HIV-1_{MM} were isolated from patients who received antiretroviral therapy for a long period of time and whose virus loads showed a number of RT and PR mutations. Two previously published CCR5 inhibitors, TAK779 and SCH-C, and zidovudine (ZDV) and saquinavar (SQV) were used as reference compounds.

45.1%]), resulting in the ratios of 1.43 and 1.40 (Fig. 5C and D), respectively. Figure 6A illustrates the overall profiles of CD4⁺/CD8⁺ cells ratios on day 16 in the four groups. The mean CD4⁺/CD8⁺ cell ratio in mice (*n* = 7) given saline was 0.1 (range, 0.06 to 0.20). In contrast, the ratios in AK602-

treated mice (*n* = 8) were significantly higher with a mean value of 0.92 (range, 0.23 to 1.89; *P* = 0.001), which was comparable to that in ddI-treated mice (*n* = 9; mean, 1.29; range, 0.38 to 2.68; *P* = 0.001) and uninfected mice (*n* = 7; mean, 1.0; range, 0.50 to 1.49). The numbers of CD4⁺ cells/μl

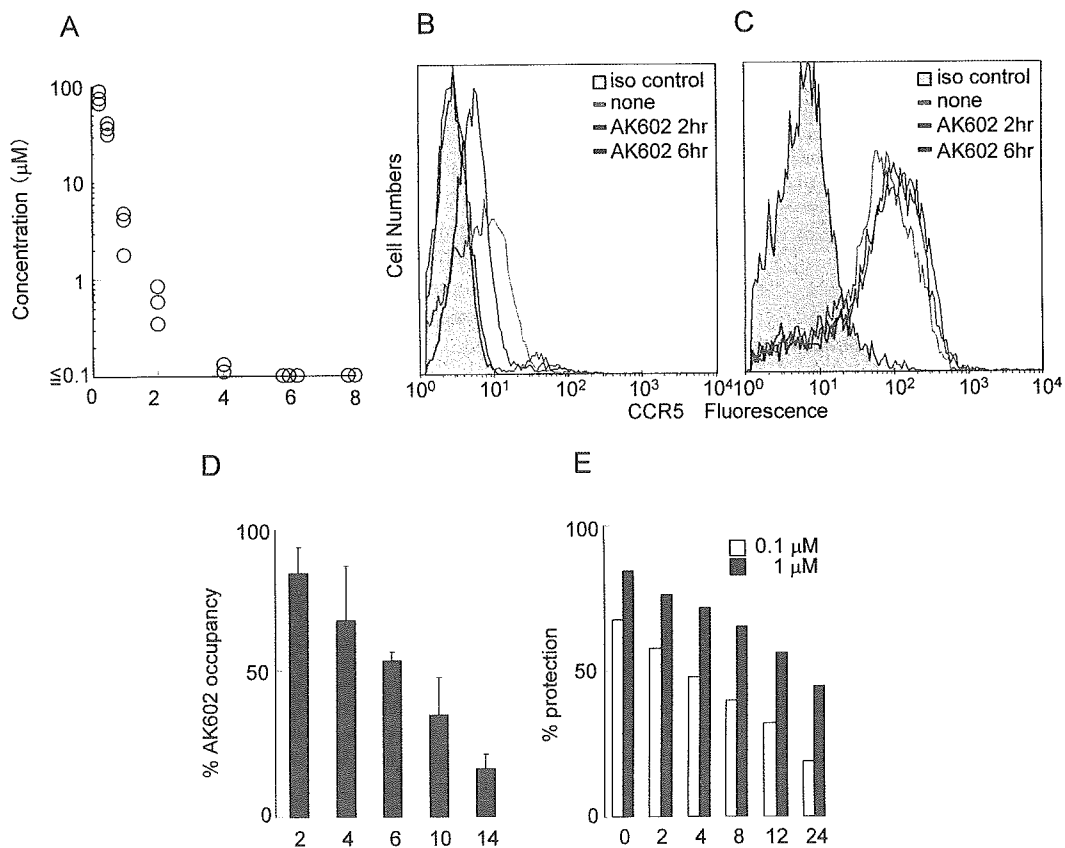


FIG. 4. Pharmacokinetics and persistence of anti-HIV-1 activity of AK602. (A) Pharmacokinetics of AK602. Each mouse was administered AK602 at a dose of 60 mg/kg, and blood samples were taken at 15, 30, 60, 120, 240, 480, and 720 min. Plasma concentrations of AK602 determined by HPLC analysis at 15, 30, 60, 120, and 240 min were 76.2, 36.1, 3.5, 0.6, and 0.13 μM, respectively. AK602 was not detected at later time points. (B and C) No CCR5 internalization or shedding was caused by AK602. Human PBMC were recovered 2 and 6 h after AK602 administration and stained with 45531 (B) or 3A9 (C). (D) Sustained AK602 occupancy on cell surfaces. At indicated periods of time after a bolus of AK-602 (60 mg/kg) was administered to hu-PBMC-NOG mice, PBMC were recovered and the percentages of AK602 occupancy on cellular CCR5 were determined with fluorescein isothiocyanate-conjugated monoclonal antibody 45531. (E) Persistence of in vitro activity of AK602 against R5 HIV-1 after AK602 depletion. CCR5⁺ MAGI cells were exposed to 0.1 or 1 μM AK602 for 30 min and thoroughly washed to deplete AK602 from the medium. The cells were subsequently cultured for the indicated periods of time, exposed to HIV-1_{Ba-L}, and further cultured for 48 h, when the cells were harvested and lysed with Triton X-100-containing PBS. A solution containing chlorophenol red-β-D-galactopyranoside was added, the optical density was measured, and the percentage of protection was determined.

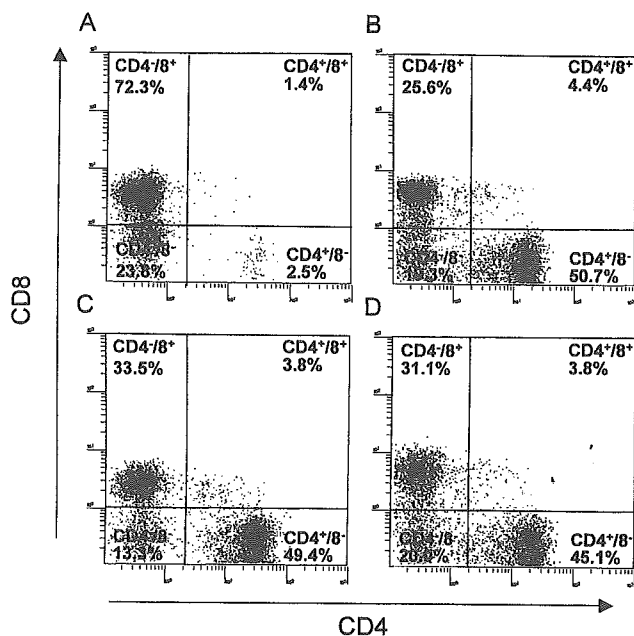


FIG. 5. Effects of AK602 on CD4⁺ and CD8⁺ cell counts in infected hu-PBMC-NOG mice. PBMC recovered on day 16 after R5 HIV-1 inoculation were subjected to flow cytometry. Shown are representative flow cytometric analysis profiles. Note that only 3.9% of CD4⁺ cells were seen (A), resulting in a CD4⁺/CD8⁺ cell ratio of 0.05 in a mouse given saline, while distinct numbers of CD4⁺ cells (55.1 and 53.2%) (B and C) were seen in AK602- and ddI-administered infected mice, resulting in CD4⁺/CD8⁺ cell ratios of 1.84 and 1.43, respectively. In an uninfected mouse (D), 48.9% of cells were positive for CD4, with a CD4⁺/CD8⁺ cell ratio of 1.40.

in saline-treated mice were significantly less than those of AK602-treated, ddI-treated, or uninfected mice (Fig. 6B).

Effects of AK602 on R5 HIV-1 proviral DNA copy numbers and serum p24 levels in R5 HIV-1-infected hu-PBMC-NOG mice. We next asked which population harbored proviral DNA in the cells recovered from R5 HIV-1-infected hu-PBMC-NOG mice, by purifying CD4⁺ and CD4⁻ cell populations and determining proviral DNA copy numbers in each population. As shown in Table 2, more than 99% of proviral DNA was found in CD4⁺ cells and <0.3% of proviral DNA was detected in CD4⁻ cells derived from saline-treated mice, indicating that R5 HIV-1 infection occurred in CD4⁺ cells in the hu-PBMC-transplanted NOG environment. As illustrated in Fig. 6C, the mean number of R5 HIV-1 proviral DNA copies was 2.0×10^5 (range, 2.6×10^4 to 1.7×10^6) per 10^5 CD4⁺ cells in R5 HIV-1-infected mice ($n = 7$) given saline. However, values for mice in groups given AK602 and ddI were 1.3×10^3 (range, 2.3×10^2 to 7.9×10^3 ; $P = 0.001$) and 1.8×10^2 (range, $<10^2$ to 7.9×10^2 ; $P = 0.001$), respectively.

The amounts of R5 HIV-1 p24 in serum were also found to be very high in saline-treated mice, with a mean amount of 1.1×10^5 pg/ml (range, 3.1×10^4 to 2.8×10^5 pg/ml). AK602 and ddI were found to significantly suppress the serum p24 amounts as examined on day 16 with a mean amount of 5.6×10^3 pg/ml (range, 8.1×10^2 to 2.1×10^4 pg/ml; $P = 0.001$) and 7.1×10^2 pg/ml (range, 1.3×10^2 to 1.1×10^4 pg/ml; $P = 0.001$), respectively (Fig. 6D).

AK602 suppressed R5 HIV-1 viremia in hu-PBMC-NOG mice. As described above, the PBMC transplanted to NOG mice were intensely activated in the xenogeneic environment and had undergone ~ 4 cycles of proliferation by day 2; a majority of the cells had undergone ≥ 10 cycles of proliferation by day 4 (Fig. 3B). These data suggested that R5 HIV-1 might extensively replicate in the hu-PBMC-NOG mice immediately after R5 HIV-1 inoculation. When we collected blood samples on days 5, 9, and 16 following the inoculation and determined R5 HIV-1 RNA copy numbers in infected, saline-treated mice ($n = 7$), the geometric mean copy number was 8.6×10^3 /ml (range, 1.7×10^3 to 1.0×10^5) on day 5 and rapidly increased to 1.9×10^5 /ml (range, 2.2×10^4 to 3.0×10^6) on day 9; by day 16, the mean copy number had reached 7.7×10^5 /ml (range, 2.6×10^5 to 3.0×10^6 /ml). However, AK602 significantly suppressed viremia by ~ 1.1 log, as examined on day 5; the mean numbers of R5 HIV-1 RNA copies in AK602-administered mice were 1.6 and 1.8 logs lower than those in saline-treated mice examined on days 9 and 16, respectively (Fig. 7). Comparable viremia suppression was seen in the mice receiving ddI (Fig. 7). It was noted that although AK602 did not completely prevent the viremia from further increasing after day 5, there was a clear reduction in the viremia increase rates. The mean slopes (change in RNA copies per day over the range of data from 5 to 16 days) for the group receiving saline was 0.167 ± 0.042 , whereas those for the AK602 and ddI groups were 0.102 ± 0.041 and 0.091 ± 0.037 , respectively. Thus, the rates of increase in the AK602 ($P = 0.0057$) and ddI ($P = 0.0023$) mice were significantly lower than that for the mice given saline, indicating that both of the agents significantly inhibited R5 HIV-1 replication in this mouse model over the range of days evaluated. No apparent AK602- or ddI-associated adverse effects were seen throughout the study period.

DISCUSSION

In the present hu-PBMC-NOG mouse model, human CD4⁺/CD8⁺ cell ratios went down to 0.1 by 16 days after R5 HIV-1 inoculation, the amounts of proviral DNA and p24 gag antigen reached 10^5 to 10^6 copies/ 10^5 CD4⁺ cells and 10^5 pg/ml, respectively (Fig. 6), and no mice failed to be infected with R5 HIV-1. It is noteworthy that the use of NOG mice provides a higher engraftment rate than with other SCID mice such as NOD/Shi-SCID mice treated with anti-NK cell antibody or the β_2 -microglobulin-deficient NOD-SCID mice (10). With NOG mice, the chimeric rate of 30 to 40% is achieved, and cord blood CD34⁺ cells have been shown to "take" with as few as 100 cells (10). Moreover, all infected mice developed high levels of R5 HIV-1 viremia by day 16, reaching as high as 10^6 copies/ml (Fig. 7). It is worth noting that the notably high levels of HIV-1 viremia seen in the present mouse model by 16 days after R5 HIV-1 exposure can be seen only on acute infection or up to 10 years after HIV infection in humans (3, 4).

In the present study, we found that the conspicuous susceptibility to the infectivity and replication of R5 HIV-1 in these mice appeared to stem from the hyperactivation of the implanted human PBMC. The implanted PBMC were highly activated in the xenogeneic environment, expressed quite high